Title: Phosphate resupply differentially impacts the shoot and root proteomes of *Arabidopsis thaliana* seedlings

Milena A. Smith[1], Lauren E. Grubb[2], Kirsten H. Benidickson[1], Devang Mehta[2,3,4], William C. Plaxton[1,5], and R. Glen Uhrig[2,6,#]

[1] Department of Biology, Queen's University, Kingston, Ontario, Canada
[2] Department of Biological Sciences, University of Alberta, Alberta, Canada
[3] Department of Biosystems, KU Leuven, Leuven, Belgium
[4] Leuven Plant Institute, KU Leuven, Leuven, Belgium
[5] Department of Biomedical and Molecular Sciences, Queen's University, Kingston, Ontario, Canada
[6] Department of Biochemistry, University of Alberta, Edmonton, Alberta, Canada

Correspondence

R. G. Uhrig, Department of Biological Sciences, University of Alberta, Edmonton, Alberta, T6G 2E9, Canada. E-mail: ruhrig@ualberta.ca

Funding Information

Queen's University Research Chair, Natural Sciences and Engineering Research Council of Canada, Canadian Foundation for Innovation

Running Title: Phosphate refeeding differentially impacts shoot and root proteomes

Abbreviations: ACP5, TYPE 5 ACID PHOSPHATASE; ALMT, aluminum-activated malate transporter; AOX, alternative oxidase; APase, acid phosphatase; BoxCarDIA,

31 BoxCar Data Independent Acquisition; DAP, differentially abundant protein; DTT,
32 dithiothreitol; FBA, fructose-bisphosphate aldolase; GABA, γ-aminobutyric acid; GAD,
33 glutamate decarboxylase; GAL, GALANTHUS NIVALIS AGGLUTININ-RELATED AND
34 APPLE DOMAIN LECTIN; GDPD1, glycerophosphodiester phosphodiesterase 1; GO,
35 Gene Ontology; GRP, glycine-rich protein; G3Pp, GLYCEROL-3-PHOSPHATE
36 PERMEASE; G6PD, glucose 6-phosphate dehydrogenase; IPS1, INDUCED BY PI
37 STARVATION; LPR, LOW PHOSPHATE ROOT; MGD, monogalactosyldiacylglycerol
38 synthase; MGDG, monogalactosyldiacylglycerol; MS, mass spectrometer; NPC4, NON-
39 SPECIFIC PHOSPHOLIPASE C4; OPPP, oxidative pentose phosphate pathway; PAH,
40 phosphatidate phosphatases; PAP, purple acid phosphatase; PCK,
41 phosphoenolpyruvate carboxykinase; PDR2, PHOSPHATE DEFICIENCY RESPONSE
42 2; PECP, Phosphoethanolamine/phosphocholine phosphatase; PEP,
43 phosphoenolpyruvate; PEPC, phosphoenolpyruvate carboxylase; PHO1,
44 PHOSPHATE1; PHR, phosphate starvation response transcription factor; PHT,
45 phosphate transporter; Pi, phosphate; -Pi, phosphate deficient; PLC2,
46 PHOSPHOLIPASE 2; PLDζ2, PHOSPHOLIPASE Dζ2; PMN, plant metabolic pathway
47 analysis; PPC, plant-type phosphoenolpyruvate carboxylase; PPi, inorganic
48 pyrophosphate; PPsPase1, inorganic pyrophosphatase-1; PSI, phosphate starvation
49 inducible; PSR, phosphate starvation response; PU, pullulanase-type limit dextrinase;
50 RNS, ribonuclease; SCL, Ser/Arg (SR)-rich and SC35-like; SDQ,
51 SULFOQUINOVOSYLDIACYLGLYCEROL; SnRK, sucrose nonfermenting1-related
52 kinase; SPS, sucrose phosphate synthase; SPX, SYG1/Pho81/XPR1; SUC, sucrose
53 transporter; T6P, trehalose-6-phospahte.
54
55

ABSTRACT

Phosphate (Pi) is an essential macronutrient for plant development that is often limited in soil environments. Plants have evolved myriad dynamic biochemical, physiological, and morphological adaptations to cope with nutritional Pi deficiency, collectively known as the Pi starvation response (PSR). While many components of the PSR have been well-characterized, much less is known about how metabolic homeostasis is re-established upon Pi resupply, particularly with respect to tissue- and time-specific adaptations. Here, we applied label-free quantitative proteomics to quantify protein-level changes in *Arabidopsis thaliana* shoots and roots following Pi resupply after prolonged Pi deprivation, quantifying a total of ~2,700 differentially abundant proteins (DAPs). Sampling at early (1 h) and late (48 h) time-points, we captured a combination of immediate signaling and metabolic responses, along with longer-term recovery processes. Early responses prioritized metabolic adjustments to restore Pi pools via enhanced glycolysis and energy production, followed by later shifts toward anabolism, including nucleotide production, membrane remodeling, and protein synthesis. Several key enzymes, including ALTERNATIVE OXIDASE 1A, FRUCTOSE-BISPHOSPHATE ALDOLASE 5, and subunits of PHOTOSYSTEM I exhibited unique tissue-specific and time-dependent regulation. Overall, our findings reveal dynamic temporal phases of metabolic reprogramming during recovery from Pi starvation, and identify candidate proteins involved in orchestrating this transition, ultimately identifying potential targets for enhancing Pi uptake- and use-efficiency in crops.

1 INTRODUCTION

Phosphorus (P) is an essential plant macronutrient required for fundamental biochemical, metabolic, and physiological processes, with root epidermal cells directly assimilating this mineral from the soil as orthophosphate ($H_2PO_4^-$; Pi) via plasmalemma Pi transporters (PHTs) (Dissanayaka *et al.*, 2021). The role of Pi in plants is multifaceted. It serves as a central structural component of important biomolecules, including nucleic acids, sugar phosphates, and phospholipids, and is also required for key processes such as photosynthesis (i.e. photophosphorylation, and triose-P exchange across chloroplast envelope) and respiration (i.e. ATP synthase of inner mitochondrial membrane). Pi also serves as an allosteric activator or inhibitor of several key regulatory enzymes of central plant metabolism, while controlling the function of many proteins via its covalent attachment to specific amino acid residues of phosphoproteins. Despite Pi's significance, most soil-Pi levels are far below those required to sustain optimal crop growth. Pi concentrations in the soil solution rarely exceed 10 μM owing to Pi's propensity to precipitate as insoluble metal cation-Pi complexes (Lambers and Plaxton, 2015). Furthermore, a significant proportion of soil-Pi is trapped in organic phosphorous (Po) compounds (i.e. decaying biomatter), which must be mineralized prior to plant uptake (Dissanayaka *et al*., 2021). Suboptimal levels of soluble Pi in soils have resulted in agricultural applications of massive quantities of unsustainable and polluting Pi fertilizers that are sourced from rapidly depleting 'rock-Pi' reserves (Dissanayaka *et al.,* 2021; Hinsinger, 2001; Blackwell *et al*., 2019). Specifically, Pi runoff from fertilized fields contaminates aquatic and marine ecosystems, triggering harmful algal and cyanobacterial blooms and eutrophication (Lambers and Plaxton, 2015). Given the inefficiency of Pi fertilizers and scarcity of rock-Pi reserves, precise agricultural solutions are urgently needed to reduce our over-reliance on exogenous Pi fertilizer application. By studying the adaptations of Pi-deficient (-Pi) plants, we may uncover potential biological targets for engineering Pi-efficient crop varieties.

Given their sessile nature, -Pi plants have evolved a variety of physiological, morphological, and biochemical adaptations that function to enhance Pi-acquisition and -use efficiency, collectively known as the Pi starvation response (PSR). The PSR is regulated by a combination of Pi-starvation inducible (PSI) genes, along with various post-

108 transcriptional and post-translational controls, ultimately increasing Pi-acquisition and -
109 use efficiency (Dissanayaka *et al.*, 2021). Given the low mobility of Pi, -Pi plants expand
110 their root networks (i.e., increased lateral root formation and root hair density) to enhance
111 foraging and thereby increase Pi-uptake (Dissanayaka *et al.,* 2021). Furthermore, PSI
112 high-affinity PHTs belonging to the PHT1 family actively transport Pi across the plasma
113 membrane of root cells against a steep concentration gradient (Dissanayaka *et al.*, 2021).
114 To mobilize soil Pi, roots of -Pi plants also excrete organic acid anions (particularly malate
115 and citrate) and Pi-scavenging enzymes (e.g., nucleases and acid phosphatases
116 (APases)) to solubilize Pi bound to metal cations and trapped in Po substrates,
117 respectively (Dissanayaka *et al.*, 2021). Plants acclimate to limiting Pi though a range of
118 Pi-sensing and scavenging mechanisms; notably, members of the PHT2-5 families
119 regulate Pi exchange and mobilization between subcellular compartments, whereas
120 secreted and vacuolar purple APases (PAPs) respectively hydrolyze Pi from extracellular
121 (i.e. cell wall, apoplast, and rhizosphere) and intracellular Pi-monoesters and anhydrides
122 (Dissanayaka *et al.*, 2021). Additionally, -Pi plants exhibit remarkable metabolic flexibility
123 by upregulating alternative enzymes to 'bypass' various adenylate- and Pi-dependent
124 reactions of central plant metabolism. For example, inorganic pyrophosphate (PPi)-
125 dependent enzymes, such as PPi-dependent phosphofructokinase, UDP-glucose
126 pyrophosphorylase, and the tonoplast H^+-PPiase have been reported to be upregulated
127 under -Pi conditions, shifting flux away from ATP-dependent pathways when cytosolic
128 ATP, but not PPi pools become significantly depleted (Palma *et al*., 2000; Dissanayaka
129 *et al*., 2021).

130 The plant PSR is governed by a complex regulatory network, with several components
131 coordinating local (i.e., Pi sensing at the root tip) and long-distance signaling
132 (Dissanayaka *et al*., 2021). During Pi-deprivation, proteins from the PHOSPHATE
133 DEFICIENCY RESPONSE 2 (PDR2) and LOW PHOSPHATE ROOT (LPR) families
134 interact to arrest primary root growth at the local level, whereas proteins containing a
135 SYG1/Pho81/XPR1 (SPX) domain modulate the PSR by binding inositol pyrophosphates
136 (Pi-signaling molecules responsive to Pi availability) (Ticconi *et al.*, 2009; Jung *et al.*,
137 2018). Notably, PHOSPHATE1 (PHO1), a xylem Pi-exporter responsible for root-to-shoot
138 Pi translocation, as well as several intracellular PHTs, contain SPX domains and are thus

139 sensitive to fluctuating Pi levels (Ham *et al.*, 2018). Plants also contain PSR transcription
140 factors (PHRs) which function as transcriptional activators of many PSI genes (Jung *et*
141 *al.*, 2018).

142 Despite identification of many PSI 'marker' genes, the complex signaling network that
143 governs the PSR is extensive, with many components remaining undiscovered. Previous
144 large-scale 'Omic' analyses focusing on plant Pi-starvation / resupply have focused on
145 comparing genetic and / or proteomic changes at discrete time-points or within a specific
146 tissue (reviewed in Zhou *et al.*, 2022). The few studies that have investigated
147 spatiotemporal PSI gene regulation reported that most are responsive following longer
148 periods of Pi starvation / recovery, although there are some 'early-response' members
149 including *TYPE 5 ACID PHOSPHATASE / PURPLE ACID PHOSPHATASE 17*
150 (*ACP5/PAP17*) and *INDUCED BY PI STARVATION 1* (*IPS1*), which are reduced in
151 transcript abundance by ~30% within 1 h of Pi-resupply (Müller *et al.*, 2004). Furthermore,
152 Hammond *et al.*, (2003) reported that the greatest proportion of both 'early'- and 'late'-
153 responsive PSI genes belonged to metabolism, cell rescue (i.e. protection from oxidative
154 stress and damage), and defense functional categories, with the proportion of genes
155 involved in transcription, protein turnover, cellular communication and transport
156 increasing in the 'late-responsive' category. Pi-sensing and gene expression also differ
157 between tissues, with root transcriptional changes preceding changes in the shoots, with
158 PSI genes being differentially expressed in different tissues, suggesting multiple
159 regulatory systems governing the PSR (Wang *et al.*, 2002; Müller *et al.*, 2004).

160 Previously, we analyzed the impact of Pi resupply on the proteome of heterotrophic -
161 Pi *Arabidopsis thaliana* (Arabidopsis) suspension cell cultures, identifying a combination
162 of previously established and novel PSI proteins (Mehta *et al.*, 2021). Here, we build on
163 this work by distinguishing both temporal- and tissue-specific response elements of the
164 PSR in Arabidopsis seedlings to gain a better understanding of its dynamic nature. With
165 proteins representing the functional units of all eukaryotic cells, quantifying proteome-
166 level changes is critical to understanding the molecular mechanisms underpinning plant
167 responses. Using quantitative proteomic approaches, we define 'early' and 'late' shoot
168 and root proteome responses to Pi-refeeding of -Pi Arabidopsis seedlings, revealing
169 several combinations of distinct and overlapping spatiotemporal proteomic changes

170 involved in diverse plant cell processes. Collectively, our global proteome analysis
171 provides critical new insights into the plant PSR to aid in the translational development of
172 crops that can better acclimate to -Pi conditions while assimilating applied Pi more
173 efficiently.
174

175 **2 MATERIALS AND METHODS**

176 **2.1 Plant Material and Treatment**

177 *Arabidopsis thaliana* Col-0 (Arabidopsis) seedlings were grown in liquid culture by
178 placing 5 mg of sterile, stratified seeds into 250 mL magenta boxes containing 50 mL of
179 sterile 0.5x Murashige-Skoog medium (pH 5.7) containing 1% (w/v) sucrose and 0.2 mM
180 Pi. Seedlings were cultivated under continuous illumination (100 µmol m^{-2} s^{-1}) at 23 ºC
181 on an orbital platform (80 rpm). After 7 days, the medium was replaced with 50 mL of
182 fresh medium containing 0 or 1.5 mM KH_2PO_4. Five days later the seedlings were either
183 supplemented with 2 mM KH_2PO_4 or maintained under -Pi; 1 and 48 h later, the Pi
184 resupplied and -Pi seedlings were harvested, rinsed with ultrapure water, and blotted dry.
185 The shoots and roots arising from each liquid culture were rapidly separated before snap
186 freezing in liquid N_2 and lyophilizing. Dry weights of lyophilized shoots and roots were
187 recorded.
188

189 **2.2 Acid Phosphatase Extraction and Activity Assays, and Protein Concentration**
190 **Determination**

191 Lyophilized shoots or roots were ground to a powder using a mortar and pestle
192 containing a small spatula of sand and homogenized (1:12; w/v for shoots, 1:30; w/v for
193 roots) in 50 mM sodium acetate (pH 5.6) containing 1 mM EDTA, 1 mM dithiothreitol
194 (DTT), 1 mM phenylmethylsulfonyl fluoride, 5 mM thiourea and 1% (w/v) insoluble
195 poly(vinylpolypyrrolidone). Homogenates were centrifuged at 14,000 x *g* for 10 min at 4
196 °C and clarified extracts were stored on ice. APase activity was measured by coupling
197 the hydrolysis of phosphoenolpyruvate (PEP) to pyruvate to the lactate dehydrogenase
198 reaction and assaying at 23 °C by monitoring NADH oxidation at 340 nm using a
199 Spectramax Plus Microplate spectrophotometer (Molecular Devices, Sunnyvale, CA,
200 USA). The APase reaction mixture contained 50 mM sodium acetate (pH 5.6), 5 mM PEP,

201 10 mM $MgCl_2$, 0.2 mM NADH, and 3 units ml^{-1} of desalted rabbit muscle lactate
202 dehydrogenase in a final volume of 0.2 ml. All assays were initiated by the addition of
203 clarified extract and corrected for any background NADH oxidation by omitting PEP from
204 the reaction mixture. One unit (U) of activity is defined as the amount resulting in the use
205 of 1 μmol min^{-1} of substrate. Protein concentrations were determined using the Bradford
206 protein assay with bovine γ-globulin as the standard.
207

208 **2.3 Tissue Processing, Proteome Extraction and Digestion**

209 Lyophilized shoots and roots were ground using Geno/Grinder (SPEX SamplePrep)
210 for 30 s at 1,200 rpm. Ground tissues were resuspended (1:2; w/v) in 50 mM Hepes-KOH
211 (pH 8.0), 100 mM NaCl, and 2% (w/v) SDS. Protein extraction was performed by shaking
212 samples at 1,000 rpm at 95 °C for 5 min using a tabletop shaker (Eppendorf ThermoMixer
213 F2.0). The samples were then clarified by centrifugation at 20,000 x *g* for 10 min at 23 °C.
214 The supernatant fluid was reduced with 10 mM DTT (Cat# D9779, Sigma) for 10 min at
215 23 °C, followed by alkylation with 30 mM iodoacetamide (Cat# I1149, Sigma) for 30 min
216 at 23 °C in the dark. Peptides were then generated using a KingFisher APEX (Thermo
217 Scientific) automated sample processing system as previously described without
218 deviation (Mehta *et al*., 2022). Here, proteins were digested using sequencing grade
219 trypsin (Cat# V5113; Promega) diluted in 50 mM triethylammonium bicarbonate buffer
220 pH 8.5 (T7408; Sigma). Samples were acidified with trifluoroacetic acid (Cat# A117,
221 Fisher) to a final concentration of 0.5% (v/v). Peptide desalting was performed as
222 previously described (Mehta *et al*., 2022) using an OT-2 liquid handling robot (Opentrons
223 Labworks Inc.) mounted with Omix C18 pipette tips (A5700310K; Agilent). Desalted
224 peptides were dried by using a speedvac at 23 °C and stored at −80 °C prior to
225 resuspension in 3.0% (v/v) acetonitrile / 0.1% (v/v) formic acid for mass spectrometer
226 (MS) injection.
227

228 **2.4 LC-MS/MS Analysis**

229 Peptides were analyzed on a Fusion Lumos Orbitrap MS (Thermo Fisher Scientific).
230 One microgram of peptide was injected per replicate using Easy-nLC 1200 system (Cat#
231 LC140; Thermo Fisher Scientific) and an Acclaim PepMap 100 C18 trap column (Cat#

232 164750; Thermo Fisher Scientific) followed by analysis using a 50 cm Easy-Spray
233 PepMap C18 analytical column (ES902; Thermo Fisher Scientific) warmed to 50 °C.
234 Peptides were eluted into the MS at 300 nL min^{-1} using a segmented solvent B gradient
235 of 0.1% (v/v) formic acid in 80% (v/v) acetonitrile (A998, Thermo Fisher Scientific) from 4
236 - 41% solvent B over 107 min as previously described (Mehta *et al*., 2022). A positive ion
237 spray voltage of 2.3 kV was used with an ion transfer tube temperature of 300 °C and an
238 RF lens setting of 40%.
239

240 **2.5 BoxCar Data Independent Acquisition (DIA)**

241 BoxCarDIA acquisition was performed as previously described, without deviation
242 (Mehta *et al*., 2022). Here, full scan MS1 spectra (350–1400 *m*/*z*) were acquired with a
243 resolution of 120,000 at 200 *m*/*z* with a normalized automatic gain control (AGC) target
244 of 100% per BoxCar isolation window and IT set to automatic. MS1 spectra were acquired
245 using two multiplexed targeted SIM scans of 10 BoxCar windows each. Fragment MS2
246 spectra were acquired at resolution of 30,000 across 28 38.5 *m*/*z* windows overlapping
247 by 1 *m*/*z* using a dynamic maximum injection time and an AGC target value of 2000%. A
248 minimum number of desired points across each peak set to 6. A summary methods file
249 has been uploaded as part of the PRIDE data repository (see Data Availability).
250

251 **2.6 Data Analysis**

252 Downstream data analysis of all acquired proteomic data was performed using
253 Spectronaut ver. 17 (Biognosys AG) with default settings as previously described (Mehta
254 *et al*., 2022). All searches were made against a custom-made decoy (reversed) version
255 of the Arabidopsis protein database from Araport 11 (27,533 protein encoding genes; ver.
256 2022-09-14). Briefly, search parameters included the following: trypsin digest permitting
257 two missed cleavages, fixed modifications (carbamidomethyl (C)), variable modifications
258 (oxidation (M)) and a peptide spectrum match, peptide and protein false discovery
259 threshold of 0.01. Significantly changing differentially abundant proteins (DAPs) were

260 determined and corrected for multiple comparisons (Bonferroni-corrected *p value* < 0.05;
261 *q value;* Table S1).
262
263 **2.7 Bioinformatics and Statistical Analysis**
264 Gene Ontology (GO) enrichment analysis was done using the Database for Annotation,
265 Visualization and Integrated Discovery (DAVID;
266 https://davidbioinformatics.nih.gov/summary.jsp). All proteins quantified within the study
267 were used as background and significance was determined based on biological
268 processes where p-value <0.01. GO dot plots were made using R version 4.3.1 and R
269 package *ggplot2*. Predicted subcellular localization of the significantly changing proteins
270 was obtained with SUBA5 and the consensus subcellular localization predictor SUBAcon
271 (https://suba.live/). Metabolic pathway analysis was performed using the Plant Metabolic
272 Network (PMN; pathway tools version 28.0; https://pmn.plantcyc.org/). Association
273 networks were generated using STRING-DB plugin (https://string-db.org/) in Cytoscape
274 version 3.10.1 (https://cytoscape.org/) and enhancedGraphics version 1.5.5
275 (https://apps.cytoscape.org/apps/) was used to generate the CIRCOS surrounding the
276 nodes. The minimum edge threshold was set 0.9 for the shoot network and 0.7 for root.
277 Statistical analyses of all proteomic data used a Bonferroni-adjusted Student's *t*-test to
278 identify significantly changing protein groups (*q-value*) unless otherwise stated. All data
279 were plotted in Graphpad Prism version 8 (https://www.graphpad.com/scientific-
280 software/prism) and Microsoft Excel, and final figures were assembled using Affinity
281 Designer software version 2.4.1 (https://affinity.serif.com/en-us/designer/).
282
283 **3 RESULTS AND DISCUSSION**
284 **3.1 Biomass and APase activity determinations validate Pi status of Arabidopsis**
285 **seedlings.**
286 Our Arabidopsis Pi starvation and re-feeding experiments were carried out using
287 seedlings initially cultured for 7 days in medium containing 0.2 mM Pi. Seedlings were
288 then transferred to Pi-deficient (20 μM) medium for 5 days, after which each seedling
289 culture was directly supplemented with either no Pi (-Pi) or 2 mM Pi (Pi-resupplied).
290 Seedlings were then harvested after either 1 or 48 h, followed by shoot and root tissue

291 lyophilization and processing for LC-MS/MS (Figure 1a). To validate the nutritional Pi
292 status of the experimental samples, we measured biomass per seedling culture following
293 lyophilization. At 48 h, the dry weight of Pi-resupplied seedling cultures was significantly
294 (40%) greater than that of -Pi seedlings (Figure 1b). At 1 h, no significant differences were
295 observed, although this is expected as changes in seedling biomass following Pi-resupply
296 are typically observed after 24-48 h (Müller *et al.*, 2004; Figure 1b).
297 A ubiquitous aspect of the plant PSR is the upregulation of secreted and vacuolar
298 PAPs, which scavenge Pi from extracellular and expendable intracellular Po compounds
299 (Veljanovski *et al.*, 2006; Dissanayaka *et al.*, 2021). We therefore assayed APase
300 activities of clarified shoot and root extracts of -Pi plants, as well as following 1 and 48 h
301 of Pi resupply. As expected, specific APase activity in the -Pi tissues was significantly
302 greater than that of the Pi-resupplied tissues at both time-points (Figure 1c and 1d). We
303 also compiled a list of over 20 PSR 'marker proteins' (i.e., those with documented
304 evidence of their involvement in the Arabidopsis PSR) that significantly changed in
305 abundance following Pi-resupply, to further validate the Pi nutritional status of our
306 samples (Table 1). Among these were several PHTs, phospholipases, PAPs, and
307 metabolic 'bypass' enzymes. In summary, our experimental model effectively induced Pi-
308 starvation conditions, followed by Pi resupply-induced recovery.
309

310 **3.2 Quantitative proteomic analysis reveals organ- and time-specific proteome**
311 **changes upon Pi resupply**

312 Quantitative LC-MS/MS was employed to analyze the shoot and root proteomes at 1 and
313 48 h following Pi-resupply. Across all treatments, ~7,000 total proteins were quantified in
314 the study, with ~2,700 found to be significantly changing differentially abundant proteins
315 (DAPs) (Log2FC > 0.58; $q \leq 0.05$) (Table 2). Of these DAPs, 483 (root) and 608 (shoot)
316 significantly changed in abundance 1 h following Pi-resupply, whereas 811 (root) and
317 1,527 (shoot) proteins significantly changed at the 48 h mark (q-value ≤ 0.05). In plotting
318 the log-transformed fold changes of these significantly changing proteins, distinct trends
319 emerge. At 1 h, the number of significantly changing DAPs increasing and decreasing in
320 abundance is approximately equal in each direction (Figure 2a). However, at 48 h
321 following Pi-resupply, 78% of root and shoot protein abundances change in tandem (i.e.

322 either positively or negatively), whereas 22% change in opposing directions (Figure 2b),
323 suggesting a temporal root-to-shoot sequence of proteome response. Furthermore, the
324 overall magnitude of protein abundance change was much greater in the 48 h Pi-
325 resupplied plants, highlighting the overall 'late-responsive' nature of recovery from Pi-
326 starvation (Müller *et al.*, 2004). At both time-points, there was a greater proportion of
327 significantly changing proteins in the shoots relative to the roots, although this difference
328 was magnified at the 48 h mark with nearly twice as many shoot proteins changing in
329 abundance relative to roots (Figure 2c). Additionally, the predicted cellular localization of
330 the significantly changing DAPs in shoots and roots at 1 and 48 h after Pi resupply
331 resolved a greater percentage of plastid-localized proteins upregulated in the shoot at 1
332 h in comparison to root and other shoot time-points (Figure S1).
333

334 **3.3 The Pi responsive proteome: previously annotated and newly discovered Pi**
335 **responsive proteins.**

336 *3.3.1 Pi sensing + transport*

337 Plants acclimate to low Pi conditions through several molecular mechanisms, including
338 the upregulation of PHTs that facilitate the uptake and transport of soil Pi to various plant
339 tissues. Among these, plasma membrane-localized PHT1s are crucial for Pi uptake at the
340 root-soil interface, with PHT1;1-1;4 contributing the most significantly of the nine PHT1
341 members found in Arabidopsis (Ayadi *et al.*, 2015). Following Pi-resupply, we observed
342 marked decreases in shoot and root PHT1;1 (AT5G43350) and PHT1;4 (AT2G38940)
343 abundance (Figure S2), the latter of which was also corroborated in our previous study
344 using Arabidopsis cell cultures (Mehta *et al.*, 2021). In contrast, PHT5;3 (AT4G22990),
345 one of the three Arabidopsis PHT5 members, was upregulated in roots following Pi-
346 resupply (Figure S2). This upregulation suggests its role in sequestering excess
347 intracellular Pi into vacuolar storage, as PHT5 proteins function as vacuolar Pi
348 transporters that help to regulate cytoplasmic Pi levels (Liu *et al.*, 2016). We also detected
349 an increase in thylakoid membrane-localized PHT4;1 (AT2G29650) 1 h following Pi-
350 resupply in the shoots (Figure S2). When grown under Pi-replete conditions, Arabidopsis
351 *pht4;1* mutants demonstrated growth defects, likely due to PHT4;1's role in chloroplast Pi
352 compartmentation and ATP synthesis (Karlsson *et al.*, 2015). These findings suggest

353 PHT4;1 may also function as an ‘early-responsive’ PSR protein, facilitating rapid Pi
354 delivery to the chloroplast stroma for ATP synthases and ultimately CO_2 fixation following
355 Pi-resupply.
356 Localization of Arabidopsis PHT1 proteins is partially coordinated by the PHOSPHATE
357 TRANSPORTER TRAFFIC FACILITATOR (AT3G52190), which is induced under Pi
358 starvation and mediates PHT1 exit from the endoplasmic reticulum (Bayle *et al.*, 2011).
359 Consistent with previous findings (Mehta *et al.*, 2021), Pi transporter traffic facilitator-1
360 abundance declined in both shoots and roots 48 h following Pi-resupply (Figure S2). In
361 contrast, we observed increased expression of PHO1;H3 (AT1G14040) (Figure S2), a
362 PHO1 homologue involved in xylem loading and root-shoot Pi translocation, thus
363 supporting shoot-targeted Pi allocation during recovery (Stefanovic *et al.*, 2011). Further
364 changes were also observed with GLYCEROL-3-PHOSPHATE PERMEASEs (G3Pp),
365 which are additional 'Pi-responsive’ transporters that regulate G3P transport to maintain
366 Pi homeostasis and redox balance (Table 1) (Ramaiah *et al.*, 2011). Notably, *G3Pp1*
367 *(AT3G47420)* demonstrates an early and sustained pattern of upregulation following Pi-
368 starvation (Misson *et al.*, 2005; Ramaiah *et al.*, 2011). Likewise, we found G3Pp1 was
369 downregulated at early and late time-points following Pi-resupply (Figure S2),
370 demonstrating its dynamic sensitivity to Pi-nutrition.
371
372 *3.3.2 Membrane lipid remodeling*
373 A hallmark of the PSR is the upregulation of hydrolytic enzymes that liberate Pi from
374 intra- and extracellular Pi-esters. Phospholipases are crucial to this process, as they
375 facilitate Pi-scavenging and membrane lipid remodeling by facilitating the replacement of
376 phospholipids with amphipathic galactolipids and sulfolipids (Dissanayaka *et al.*, 2021).
377 In our study, several phospholipases were significantly downregulated following Pi
378 resupply in both shoots and roots, including NON-SPECIFIC PHOSPHOLIPASE C4
379 (NPC4; AT3G03530), PHOSPHOLIPASE 2 (PLC2; AT3G08510), PHOSPHOLIPASE
380 Dζ2 (PLDζ2; AT3G05630), and glycerophosphodiester phosphodiesterase 1 (GDPD1;
381 AT3G02040) (Figure S2) indicating a shift in lipid metabolism as the plants adjust to the
382 restored Pi levels. NPC4 belongs to the NPC protein family, which hydrolyze
383 phospholipids to produce diacylglycerol (DAG) and a phosphorylated head group (Yang

384 *et al.*, 2021). Upon Pi starvation, *npc4* knockout plants exhibit impaired
385 phosphatidylcholine hydrolysis and reduced root hair elongation (Nakamura *et al.*, 2005;
386 Su *et al.*, 2018; Yang *et al.*, 2021). PLC2, although less well characterized in the context
387 of Pi nutrition, has been implicated in stress signaling, including drought tolerance,
388 pathogen defense, and auxin-regulated root growth (Georges *et al.*, 2009; D'Ambrosio *et*
389 *al.*, 2017; Chen *et al.*, 2019; van Hooren *et al.*, 2024). Its downregulation suggests a
390 broader role in Pi-associated stress signaling and lipid remodeling. PLDζ2 functions within
391 the plant PSR to facilitate phosphatidylcholine hydrolysis to yield Pi (Su *et al.*, 2018).
392 Interestingly, the Arabidopsis *PLDζ2* promoter contains an evolutionarily conserved Pi
393 starvation-responsive transcriptional enhancer, which enhances root phospholipid
394 degradation during Pi deficiency (Oropeza-Aburto *et al.*, 2012). Additionally, *pldζ2*
395 knockout plants demonstrate reduced galactolipid replacement of membrane
396 phospholipids during Pi-starvation (Su *et al.*, 2018). GDPD1 hydrolyzes
397 glycerophosphodiesters into glycerol-3-P and alcohol to liberate Pi and is transcriptionally
398 induced during Pi starvation via PHR1-binding promoter elements in a time-dependent
399 manner (Cheng *et al.*, 2011). Our analysis determined that GDPD1 was strongly
400 downregulated in all tissues and timepoints, complementing the results of Cheng *et al*.
401 (2011) which supports its status as a dynamic PSR marker.

402 Sulfolipid replacement of phospholipids, an additional Pi-conserving strategy, requires
403 the biosynthesis of sulfoquinovosyldiacylglycerol via two sulfolipid biosynthesis proteins,
404 SULFOQUINOVOSYLDIACYLGLYCEROL 1 (SQD1; AT4G33030) and SDQ2
405 (AT5G01220). SQD1 converts UDP-glucose and sulfite into UDP-sulfoquinovose, a
406 sulfolipid biosynthetic precursor, whereas SQD2 transfers this sulfoquinovose to DAG,
407 forming sulfoquinovosyldiacylglycerol (Yu *et al.*, 2002). We found both enzymes were
408 downregulated 48 h following Pi resupply (Figure S2), consistent with previous findings
409 that demonstrate their critical role in the PSR (Essigmann *et al.*, 1998; Yu *et al.*, 2002;
410 Okazaki *et al.*, 2009).

411 Plants also conserve Pi by substituting phospholipids with glycolipids such as
412 monogalactosyldiacylglycerol (MGDG), synthesized by MGDG synthases (MGD1–3).
413 MGD1 is the primary isozyme involved in bulk MGDG synthesis necessary for rapid
414 membrane thylakoid expansion, whereas MGD2 and MGD3 play a more specialized role

415 under Pi-limiting conditions, particularly in non-photosynthetic tissues (Awai *et al.*, 2001;
416 Kobayashi *et al.*, 2009; Nitenberg *et al.*, 2020). Our data revealed MGD1 (AT4G31780)
417 was significantly downregulated in the shoots 48 h following Pi-resupply, whereas MGD3
418 (AT2G11810) was downregulated in both tissues at 1 h and in the shoots at 48 h (Figure
419 S2). Although not previously linked to Pi-nutrition, MGD1 is sensitive to aluminum stress,
420 likely due to its role(s) in lipid transport (Liu *et al.*, 2020). As aluminum precipitates soil Pi
421 and binds to negatively charged phospholipids in the plasma membrane, aluminum stress
422 is often linked to Pi starvation; perhaps MGD1 has overlapping roles in mitigating
423 aluminum toxicity and Pi starvation in plants (Panda and Matsumoto, 2009; Liu *et al.*,
424 2020). MGD3 has been designated as a 'fast responder' to Pi-resupply, as demonstrated
425 by its rapid transcriptional repression within 30 min of Pi-resupply in Arabidopsis roots
426 (Hanchi *et al.*, 2018). Furthermore, -Pi Arabidopsis *mgd3* mutants displayed drastic
427 reductions in root glycolipid accumulation, fresh weight, root growth, and photosynthetic
428 capabilities (Kobayashi *et al.*, 2009). Our protein-level data reinforce MGD3's dynamic
429 and temporal involvement in plant Pi-recovery. Notably, neither MGD1 nor MGD3 were
430 detected in Pi-resupplied Arabidopsis cell cultures (Mehta *et al.*, 2021), highlighting the
431 importance of a whole-plant tissue context.

432 Phosphatidate phosphatases (PAHs) hydrolyze membrane-bound phosphatidic acid
433 for subsequent production of DAG (i.e., galactolipid precursor). Arabidopsis PAH1
434 (AT3G09560) and PAH2 (AT5G42870) are hypothesized to be a limiting step in Pi
435 starvation-induced lipid remodeling; Arabidopsis *pah1pah2* double mutants demonstrated
436 severe reductions in galactolipid production, elevated phospholipid content, impaired
437 growth under N-deficiency, and heightened aluminum sensitivity under -Pi conditions
438 (Nakamura *et al.*, 2009; Kobayashi *et al.*, 2013; Yoshitake *et al.*, 2017). We detected a
439 shoot-specific decrease in PAH1/2 abundance following 48 h of Pi-refeeding (Figure S2),
440 suggesting a role in photosynthetic (i.e., chloroplast) membrane DAG production and
441 subsequent MGD1 galactosylation for phospholipid membrane replacement (Nakamura
442 *et al.*, 2009). This is further evidenced by the lack of PAH1/2 identification in *Arabidopsis*
443 cell cultures (Mehta *et al.*, 2021), suggesting a Pi-starvation/resupply induced regulatory
444 mechanism specific to autotrophic tissues.

445 Phosphoethanolamine / phosphocholine phosphatase 1 (PECP1; AT1G17710) and
446 inorganic pyrophosphatase-1 (PPsPase1; AT1G73010) are well-established markers of
447 Pi starvation that dephosphorylate phospholipid head groups to recycle Pi (Table 1)
448 (Hanchi *et al.*, 2018; Tannert *et al.*, 2018; Angkawijaya *et al.*, 2019). Following Pi-
449 resupply, both phosphatases were strongly downregulated at 1 h (Figure S2),
450 corroborating previous transcriptional evidence demonstrating a rapid (within 30 min)
451 decrease in *PECP1* and *PPsPase1* mRNAs following Pi-replenishment (Hanchi *et al.*,
452 2018). Given their dynamic expression in response to Pi availability, these phosphatases
453 serve as sensitive 'reporters' of Pi starvation.
454
455 *3.3.3 Pi scavenging*
456 Organic phosphorus (Po) compounds, such as nucleic acids derived from decaying
457 biomatter, constitute 30–90% of the soil's phosphorous pool (Dissanayaka *et al*., 2021).
458 Likewise, endogenous nucleic acids account for nearly 50% of cellular Po of Pi-sufficient
459 plants, with rRNA comprising 80% of this pool (Stigter and Plaxton, 2015). A hallmark of
460 the plant PSR is the upregulation and root secretion of nucleases, ribonucleases
461 (RNases), phosphodiesterases, and PAPs to liberate Pi from Po compounds
462 (Dissanayaka *et al.*, 2021). RNases are ubiquitous enzymes that maintain RNA
463 degradation and turnover, and their Pi recycling abilities have been well-characterized in
464 several plant species, including Arabidopsis, tomato, *Nicotiana alata*, rice, and
465 snapdragon (Taylor *et al.*, 1993; Köck *et al.*, 1998; Bariola *et al*., 1999; Liang *et al.*, 2002;
466 Rojas *et al*., 2013; Gho *et al.*, 2020). Arabidopsis ribonuclease 2 (RNS2) (AT2G39780) is
467 constitutively expressed to mediate vacuolar RNA degradation and recycling, although its
468 expression is further induced during Pi starvation or senescence to remobilize Pi (Taylor
469 *et al.*, 1993; Bariola *et al*., 1999; Liu *et al*., 2025). We found RNS2 was downregulated in
470 shoots after 48 h of Pi-resupply (Figure S2), reinforcing its Pi-sensitivity. Interestingly, we
471 found RNS3 (AT1G26820) was moderately downregulated in roots at 1 h and strongly
472 downregulated in shoots at 48 h (Figure S2). RNS3, a secreted RNase, is typically
473 induced by senescence rather than Pi starvation (Taylor *et al.*, 1993; Bariola *et al.*, 1994;
474 Bariola *et al*., 1999). Given this discrepancy, perhaps RNS3 plays a more nuanced role
475 with respect to Pi-recovery (rather than Pi-starvation) as the requirement for extracellular

476 RNases rapidly decreases upon Pi-resupply. Furthermore, this discovery along with the
477 lack of RNS2/3 detection in Arabidopsis cell cultures (Mehta *et al.*, 2021) highlights the
478 complex overlap between senescence and Pi-responsive signal transduction networks
479 within various plant tissues (Dissanayaka *et al.*, 2021).

480 APases hydrolyze Pi from organic Pi-monoesters and their upregulation is a distinctive
481 feature of the plant PSR. PAPs are the largest class of plant APases, with the Arabidopsis
482 genome encoding 29 different PAP isozymes that exhibit unique expression, localization,
483 and metabolic patterns (Tran *et al*., 2010). Here, we found 13 PAPs were downregulated
484 following Pi-resupply, and of these 13, PAP10, PAP12, PAP14, PAP17, PAP24, and
485 PAP25 were also discovered in Arabidopsis cell cultures (Figure S2) (Tran *et al*., 2010;
486 DelVecchio *et al*., 2014; Mehta *et al.*, 2021; O'Gallagher *et al*., 2022). Previous literature
487 has thoroughly characterized PAP10, PAP12, PAP17, PAP25, and PAP26 as the major
488 Pi-responsive PAPs, as they are strongly upregulated at transcript and/or protein level
489 during Pi deprivation (Del Pozo *et al.*, 1999; Hurley *et al.*, 2010; Tran *et al.*, 2010; Wang
490 *et al.*, 2011; Robinson *et al.*, 2012a; Robinson *et al.*, 2012b; Wang *et al.*, 2014; Del
491 Vecchio *et al.*, 2014; Zhang *et al.*, 2014; Ghahremani *et al.*, 2019; O'Gallagher *et al.*,
492 2022). Furthermore, PAP12 and PAP26 are the main root-secreted and cell wall targeted
493 APases that scavenge Pi from extracellular Pi-esters, while the dual-targeted AtPAP26
494 functions as the dominant vacuolar APase (Hurley *et al.*, 2010; Robinson *et al*., 2012; Liu
495 *et al*., 2025). Consistent with Mehta *et al.* (2021), PAP17 was the most downregulated
496 PAP (in both tissues) following Pi resupply, underscoring its tight regulation during Pi-
497 deprivation or leaf senescence (O'Gallagher *et al.*, 2022). Interestingly, PAP27 was the
498 only PAP downregulated at the 1 h resupply time-point, suggesting an 'early-responsive'
499 role. Beyond Pi-starvation, PAP27 is also sensitive to pathogen infection and zinc
500 deficiency (a condition with a well-established connection to Pi), hinting at a broader role
501 in stress signaling (van de Mortel *et al.*, 2006; Ascencio-Ibáñez *et al.*, 2008; Khan *et al.*,
502 2014).

503 Arabidopsis GALANTHUS NIVALIS AGGLUTININ-RELATED AND APPLE DOMAIN
504 LECTIN-1 (GAL1), a dual-localized (cell wall and vacuole) mannose-binding lectin,
505 interacts with a high mannose-glycoform of PAP26 to enhance its APase activity and
506 stability to facilitate Pi scavenging during Pi starvation (Ghahremani *et al.*, 2019;

507 Ghahremani *et al.*, 2019). Moreover, GAL1 was reported to be upregulated following Pi-
508 but not phosphite-resupply in Arabidopsis cell cultures, suggesting a Pi-specific recovery
509 response. While GAL1 is induced under Pi starvation (Ghahremani *et al.*, 2019a), we
510 found that its closest paralog, GAL2 (AT1G78860), was strongly upregulated following Pi
511 resupply (Figure S2). This divergence in expression patterns could perhaps indicate these
512 paralogs possess differential roles within the PSR, though more work is needed to explore
513 GAL2's unique role in Pi-recovery.
514
515 *3.3.4 Metabolic 'bypass' enzymes*
516 Extended Pi starvation in plants depletes vacuolar Pi reserves, leading to reduced
517 cytoplasmic Pi and Po levels (Dissanayaka *et al.*, 2021). As several glycolytic enzymes
518 rely on Pi-containing adenylates or Pi as a co-substrate, -Pi plants demonstrate significant
519 metabolic and physiological impairments; however, they also possess remarkable
520 metabolic redundancy, allowing them to bypass these steps through alternative adenylate
521 and Pi-independent pathways. Plants upregulate several enzymes that utilize PPi as a
522 co-substrate, which in contrast to Pi, ATP, and ADP is unaffected by Pi-deprivation (Duff
523 *et al*., 1989). During Pi deprivation PEP carboxylase (PEPC) is simultaneously
524 upregulated and activated by phosphorylation (Duff *et al.,* 1989, Gregory *et al*., 2009;
525 Masakapalli *et al.*, 2014; Mehta *et al*., 2019). In tandem with NAD-malate dehydrogenase
526 and NAD-malic enzyme PEPC provides an ADP-independent bypass to pyruvate kinase,
527 thus maintaining pyruvate availability for mitochondrial respiration while recycling Pi (a
528 PEPC byproduct) under Pi-limiting conditions. Intermediate products of this bypass
529 pathway include malate, which along with other carboxylates such as citrate is excreted
530 by roots to mobilize Pi from the insoluble metal cation-Pi complexes in the soil
531 (Dissanyanka *et al.,* 2021). Arabidopsis plant-type PEPC isozymes (PPC) 1–3 are Pi-
532 responsive enzymes that are upregulated and activated by phosphorylation during Pi
533 starvation (Gregory *et al.*, 2009; Feria *et al.*, 2016). Likewise, we found PPC2
534 (AT2G42600) and PPC3 (AT3G14940) were downregulated 48 h following Pi-resupply in
535 both shoots and roots, while PPC1 (AT1G53310) decreased only in shoots (Figure S2).
536 Interestingly, we found two isozymes of PEP carboxykinase (PCK1, AT4G37870; PCK2,
537 AT5G65690), which catalyze the reverse reaction of PEPC, (i.e., oxaloacetate

538 decarboxylation to PEP) were upregulated in shoots 48 h following Pi-resupply (Figure
539 S2) (Rojas and Iglesias, 2023). To the best of our knowledge, no studies have
540 characterized PCK as being Pi-responsive, although perhaps its Pi-resupply mediated
541 upregulation suggests the point at which gluconeogenesis is reinitiated, converting stored
542 carbon (e.g., malate) into PEP for sugar synthesis and restoration of anabolic growth post
543 -Pi recovery (Dissanayaka *et al.*, 2021).

544 Additionally, the oxidative pentose phosphate pathway (OPPP) is proposed to be a Pi
545 recovery-inducible pathway due to its dual role in producing carbon precursors for
546 macromolecule synthesis, and for restoring redox balance (i.e., NADPH production) when
547 cell transitions from a stress-induced, quiescent metabolic state to a growth-promoting
548 anabolic state (Mehta *et al.*, 2021; Smith *et al.*, 2024). Within this pathway, we found 6-
549 phosphogluconolactonase-1 (AT1G13700) and glucose 6-P dehydrogenase 1 (G6PD1;
550 AT5G35790) were upregulated following Pi-resupply (Figure S2). The latter finding
551 corroborates that of Yin and Ashihara (2008), who reported rapid *G6PD1* upregulation 24
552 h following Pi refeeding of Arabidopsis cell cultures. Given that G6PD catalyzes the first
553 committed step of the OPPP pathway, perhaps this 'fast-responsive' upregulation is
554 required to jumpstart metabolic flux through this pathway to support the rapid resumption
555 of cell growth that ensues upon Pi resupply.

556 We also found both glutamate decarboxylase (GAD) 1 (AT5G17330) and 4
557 (AT2G02010) were downregulated in the shoots 48 h following Pi-resupply (Figure S2).
558 GAD represents a branchpoint enzyme that mediates flux through the γ-aminobutyric acid
559 (GABA) shunt, a tricarboxylic acid cycle bypass that helps drive mitochondrial respiration
560 under stress conditions (Brown and Shelp, 2016). GAD1 has been hypothesized to
561 upregulate GABA shunt flux during Pi-deprivation to circumvent thiamine diphosphate-
562 dependent 2-oxoglutarate dehydrogenase activity, thus maintaining tricarboxylic acid
563 cycle flux and cell respiration (Benidickson *et al.*, 2023). This is evidenced by
564 hyperphosphorylation of GAD1's N-terminus following Pi-resupply of -Pi Arabidopsis cell
565 cultures, phenotypic impairments in -Pi *atgad1* mutants compared to wild-type plants, as
566 well as GAD1 transcript and polypeptide upregulation in -Pi shoots (Mehta *et al.*, 2021;
567 Benidickson *et al.*, 2023). GABA is also known to modulate aluminum-activated malate
568 transporter (ALMT) activity; notably, ALMT3 localizes to root hair membranes during Pi-

569 starvation to mediate malate efflux for soil-Pi liberation (Ramesh *et al.*, 2015; Gilliham
570 and Tyerman, 2016; Maruyama *et al.*, 2019). Interestingly, ALMT9 (AT3G18440), a
571 malate-activated chloride channel involved in drought responses and stomatal aperture
572 regulation, demonstrated the greatest change in abundance across our dataset,
573 decreasing notably in both tissues following Pi resupply (Figure S2) (De Angeli *et al.*,
574 2013). ALMT9 is also implicated in GABA-mediated stomatal signaling (Xu *et al.*, 2021;
575 Gilliham and Xu, 2022; Jaślan and De Angeli, 2022), suggesting a potential but
576 unexplored role in Pi-related GABA signaling.

577 Pi deprived plants can also bypass the Pi- and ADP-dependent reactions of
578 mitochondrial respiration (i.e., ATP synthases) via alternative oxidase (AOX). AOX
579 minimizes the production of toxic reactive oxygen species by maintaining electron flow
580 through the mitochondrial electron transport chain (from ubiquinone to O_2) when electron
581 flux through the energy-conserving cytochrome pathway is restricted by the low
582 intracellular ADP and Pi levels that accompany prolonged Pi starvation (Parsons *et al.*,
583 1999; Dissanayaka *et al.*, 2021). In our study, AOX1A (AT3G22370) and AOX1D
584 (AT1G32350) showed mixed responses to Pi-resupply (Figure S2). Previous work has
585 demonstrated AOX1A is upregulated by Pi starvation and downregulated upon Pi
586 resupply in Arabidopsis (Hammond *et al.*, 2003; Vijayraghavan and Soole, 2010; Mehta
587 *et al.*, 2021). Interestingly, we observed divergent regulation of AOX1A between shoots
588 and roots, along with a strong, early downregulation of AOX1D in the roots; these
589 regulatory differences point to the complex, intricate metabolic flexibility that accompanies
590 Pi starvation/resupply.

591

592 **3.4 Gene Ontology and Network Analysis Identify Novel Biological Processes**
593 **Impacted Upon Pi Resupply**

594 In addition to known Pi-responsive markers, we were interested in identifying what
595 other biological processes may be impacted at the proteome-level upon Pi resupply. To
596 this end, we first performed a Gene Ontology (GO) enrichment analysis using the proteins
597 that were significantly down- or upregulated upon Pi resupply at both 1 and 48 h time-
598 points in root and shoot (Figure 3a and 3b). In correlation with the observed Pi markers
599 mentioned above, the analysis identified enrichment of ‘Cellular Response to Phosphate

600 Starvation' (GO:0016036) among downregulated proteins in both shoots and roots at 48
601 h, as well as 'Phospholipid Metabolic Process' (GO:0006644) downregulated in root, and
602 'Glycolipid Biosynthetic process' (GO:0009247) downregulated in shoot, both at 48 h. We
603 additionally noted enriched GO terms related to mRNA splicing among both root and
604 shoot downregulated proteins, as well as a strong enrichment of GO terms relating to
605 translation among upregulated proteins in shoot. To further define biological processes
606 that may be impacted by the Pi resupply, we performed a STRING-DB association
607 network analysis for both our shoot and root changing proteome (Figure 4). Protein
608 association networks exhibiting significant changes in abundance under Pi-resupply
609 treatments were created based on the StringDB database. As expected, both the shoot
610 and root association networks showed a clear grouping of proteins primarily
611 downregulated at 48 h with relation to Pi transport and metabolism as well as phospholipid
612 metabolism. In addition, we observed nodes pertaining to the spliceosome, showing
613 mostly downregulation at 48 h in root, with less of a clear pattern in shoot. Similarly, a
614 grouping of proteins related to starch and sucrose metabolism showed a clear pattern of
615 downregulation at 48 h in both shoot and root networks. One of the most striking patterns
616 we observed among the association network was the clear upregulation of proteins
617 involved in translation and ribosome biogenesis in shoots at 48 h of Pi resupply. Finally,
618 we noted some differential regulation of photosynthesis-related proteins at the two time-
619 points, with mostly upregulation at 1 h, followed primarily by downregulation at 48 h
620 following Pi resupply. Next, we queried our data for metabolic pathways that may be
621 significantly enriched, undertaking a plant metabolic pathway analysis (PMN; Table S2).
622 In line with our GO and association network analyses, this strengthened the observation
623 of changes in phospholipid and glycolipid metabolism, photosynthesis, carbohydrate
624 metabolism and phenylpropanoid metabolism.
625

626 *3.4.1 Translation and RNA splicing*

627 Of all the categorized processes, the largest pool of significantly changing proteins
628 (i.e., increased abundance) belonged to the ribosome biogenesis/translation network,
629 particularly in the 48 h shoots (Figures 3 and 4). This large upregulation of protein
630 synthesis machinery is expected, given Pi-starvation leads to an arrest in plant growth

631 (and consequently down regulated protein synthesis), and a substantial proportion of
632 cellular Pi is dedicated to rRNA (Wu *et al.*, 2003; Veneklaas *et al.*, 2012). In particular,
633 the Arabidopsis ribosome biogenesis regulatory protein (RRS1) which directly modulates
634 ribosome biogenesis was dramatically upregulated in the 48 h shoots (AT2G37990; 48 h
635 shoot, +7.7169 Log2FC; 48 h root, +1.3912 Log2FC) (Choi *et al.*, 2005).
636 Our data also identified mRNA splicing as downregulated in both tissues, though more
637 so at 1 h in shoots and 48 h in roots (Figures 3 and 4). Several of these downregulated
638 proteins were alternative splicing factors, particularly Ser/Arg (SR)-rich and SC35-like
639 (SCL) proteins, which are involved in plant abiotic and nutritional stress responses (Chen
640 *et al.*, 2013; Zhang *et al.*, 2014; Dong *et al.*, 2018). In particular, several rice SR/SCL
641 genes are involved in Pi homeostasis; two of which, SCL30/30a
642 (Os12g38430/Os02g15310) and SR33 (Os07g0673500) have confirmed homology with
643 Arabidopsis SCL30 (AT3G55460) and SR34 (AT1G02840), respectively, and were also
644 downregulated in our study (AtSCL30; Shoot 1 h, -1.248 Log2FC, Shoot 48 h, -1.100
645 Log2FC, Root 48 h, -0.644 Log2FC; AtSR34; Root 48 h, -0.822 Log2FC) (Iida and Go,
646 2006; Dong *et al.*, 2018; Gao *et al.*, 2023). Furthermore, alternative splicing of
647 REGULATOR OF LEAF INCLINATION 1 which modulates rice shoot architecture
648 produces two protein isoforms that directly control PSR signaling pathways (Guo *et al.*,
649 2022). Taken together, the PSI decrease in protein synthesis is likely a coordinated effect
650 of decreased ribosome biogenesis coupled with increased alternative splicing.
651
652 *3.4.2 Carbohydrate Metabolism*
653 Carbohydrate (i.e., starch and sucrose) metabolism enzymes in shoots was mostly
654 downregulated at 48 h, although this response was varied in roots (Figures 3b and 4). In
655 general, enzymes were upregulated that support anabolic growth, including G6PD1
656 involved in C-skeleton and nucleotide synthesis (discussed above) and ISOCITRATE
657 LYASE (AT3G21720), a key enzyme of the glyoxylate cycle (Table S1). Several cell wall
658 pectin/starch synthesis enzymes were also upregulated, including UDP-D-glucuronate 4-
659 epimerase 1, 5, and 6 (Table S1), galacturonosyltransferase 1 (AT3G61130; root 48 h,
660 +0.967 Log2FC), and PROTEIN TARGETING TO STARCH (AT5G39790; root 48 h
661 +1.042 Log2FC). Contrary to this, enzymes related to C metabolism involved in the PSR

662 were downregulated: sucrose-P synthase (SPS), a key enzyme involved in sucrose
663 production, was downregulated in 48 h Pi-resupplied shoots and roots (SPS1F;
664 AT5G20280; Root 48 h, -0.7756 Log2FC; SPS2F; AT5G11110; Shoot 48 h, -0.628
665 Log2FC, Root 48 h -0.8478 Log2FC; SPS4F; AT4G10120; Shoot 48 h, -1.096 Log2FC,
666 Root 48 h, -0.8759). A characteristic early response of the PSR is the production of
667 sucrose, which is a global regulator of Pi starvation signaling (Hammond and White, 2008;
668 Lei *et al.*, 2011). Furthermore, we found sucrose transporter 2 (SUC2) was downregulated
669 in 48 h root tissues (AT2G02860; -0.8322 Log2FC). SUC2 facilitates root-sucrose
670 transport, thus signaling the activation of Pi-responsive genes; disruption of the *SUC2*
671 gene greatly inhibits plant PSR mechanisms (Lei *et al.*, 2011).
672
673 3.4.3 Phenylpropanoid metabolism
674 Under Pi starvation, phenylpropanoid biosynthesis is induced as they contribute to
675 defense and structural modifications, including changes to root architecture (Luo *et al.*,
676 2021; Wang *et al.*, 2021). Correspondingly, we found phenylpropanoid biosynthesis was
677 largely downregulated in shoot tissue following Pi resupply (Figure 4b). In particular,
678 several enzymes involved in anthocyanin biosynthesis were downregulated, including
679 leucoanthocyanidin dioxygenase (AT4G22880; Shoot 48 h -1.808 Log2FC), chalcone
680 synthase (AT5G13930; Shoot 48 h -1.426 Log2FC), and flavonol synthase 5
681 (AT5G63600; Shoot 1 h -1.325 Log2FC). Leaf anthocyanin accumulation is a
682 characteristic component of the plant PSR, as it protects against photoinhibitory damage
683 during Pi-limited photosynthesis, whilst serving as metabolic markers of nutrient
684 deficiency as seen by the classic purple pigmentation of -Pi plant leaves (Dissanayaka *et*
685 *al.*, 2021; Li *et al.*, 2023). Previous evidence has identified leucoanthocyanidin
686 dioxygenase as part of the plant PSR as its promoter contains PHR1 binding motifs (Liu
687 *et al.*, 2022). Chalcone synthase can also be linked to the PSR, as its expression is
688 regulated by the Arabidopsis PRODUCTION OF ANTHOCYANIN PIGMENTS1
689 transcription factor; a Pi starvation-inducible regulator of anthocyanin biosynthesis (Li *et*
690 *al.*, 2016; Tao *et al.*, 2024).
691
692 *3.4.4 Photosynthesis*

693 In shoots, a major point of opposing regulation between the Pi-resupply timepoints was
694 photosynthesis (i.e., photosynthetic proteins), which was generally upregulated at 1 h and
695 downregulated at 48 h (Figures 3c and 4b; Supplemental Figure S1). As Pi is critical for
696 ATP production and immediate restoration of metabolic homeostasis, we would expect a
697 transient upregulation of photosynthetic machinery immediately following Pi
698 supplementation (Carstensen *et al.*, 2018). As sugar stores are replenished, there is a
699 metabolic shift from photosynthetic recovery to other anabolic Pi-dependent processes,
700 such as nucleotide synthesis, membrane rebuilding, and growth (Smith *et al.*, 2024).
701 Furthermore, prolonged leaf illumination without an adequate supply of Pi leads to
702 photoinhibition and ROS production. Some specific photosynthetic proteins that followed
703 this pattern were photosystem I subunits O, D1, and G (AT1G08380, AT4G02770, and
704 AT1G55670 respectively), which were all upregulated at 1 h and downregulated at 48 h
705 in shoots (Table S3). Interestingly, the dihydrolipoamide branched chain acyltransferase
706 BCE2 had one of the most dramatically different regulatory patterns in shoots between
707 timepoints (AT3G06850; 1 h, +3.35 Log2FC; 48 h, -5.48 Log2FC). BCE2 is a multifaceted
708 protein that is induced during sucrose starvation, senescence/darkness, and in plants
709 with impaired photosynthetic function (via mutation of the Thr78 phosphorylation site of
710 rubisco activase) (Fujiki *et al.*, 2005; Binder *et al.*, 2007; Arias *et al.*, 2014; Kim *et al.*,
711 2019). Given sucrose accumulation and signaling are major regulators of the plant PSR,
712 perhaps a rapid decrease in cytosolic sucrose levels following Pi-resupply (partially via
713 direct allosteric inhibition of sucrose-P synthase by Pi) triggered an immediate
714 upregulation of BCE2, followed by its downregulation at 48 h as sucrose and Pi levels
715 stabilize (Doehlert and Huber, 1984; Lei *et al.*, 2011). It would be of significance to explore
716 BCE2's putative role(s) in connecting Pi nutrition, sucrose signaling, and senescence.
717 In line with the regulatory pattern of photosynthetic proteins, two proteins involved in
718 carbohydrate metabolism, fructose-bisphosphate aldolase 5 (FBA5; AT4G26530) and
719 pullulanase-type limit dextrinase 1 (PU1; AT5G04360) were upregulated at 1 h then
720 downregulated at 48 h (FBA5; shoot 1 h, +0.584 Log2FC, shoot 48 h, -0.795 Log2FC;
721 PU1; root 1 h, +0.664 Log2FC, root 48 h, -2.34 Log2FC, shoot 48 h, -0.736 Log2FC).
722 FBA5 is a cytosolic glycolytic intermediate that catalyzes fructose-1,6-P_2/triose-P
723 interconversion and is bound by calmodulin in a Ca^{2+}-dependent manner (Symonds *et*

724 *al.*, 2024), whereas PU1 catalyzes the hydrolysis of the α-1,6 linkages of amylopectin
725 during starch degradation, thus liberating glucose for glycolysis (Delatte *et al.*, 2006;).
726 Upon replenished Pi stores, the immediate upregulation of these enzymes would
727 simultaneously yield glucose and enhance glycolytic and respiratory flux for ATP
728 production, followed by a shift towards anabolic growth at 48 h once energy reserves are
729 restored.

730 In roots, the glycine-rich protein 3 (GRP3) was downregulated at 1 h, followed by a
731 dramatic upregulation at 48 h (AT2G0552; Root 1 h, -1.22 Log2FC, Root 48 h, +5.05
732 Log2FC). GRP3 is a repressor of cell elongation, as demonstrated by increased root
733 growth in *atgrp3* knockout plants, whose expression is induced by trehalose-6-P (T6P)
734 (Schluepmann *et al.*, 2004; Mangeon *et al.*, 2016). Furthermore, GRP3 functions in the
735 Arabidopsis wall-associated kinase 1-mediated aluminum signaling pathway, which may
736 be connected to the PSR signaling pathway given the overlap between aluminum and Pi-
737 stress response mechanisms (Sivaguru *et al.*, 2003; Chen *et al.*, 2022). The dynamic
738 regulation of GRP3 likely mirrors cellular sucrose levels and T6P-mediated control of
739 carbohydrate metabolism following Pi-resupply; elevated sucrose levels immediately
740 following Pi-resupply result in increased conversion of G6P and UDP-Glucose to T6P by
741 trehalose-6-P synthase, thus inhibiting sucrose nonfermenting1-related kinase1 (SnRK1)
742 to promote growth (Müller *et al.*, 2004; Schluepmann *et al.*, 2004; Smeekens, 2015). After
743 48 h, the decline in sucrose levels facilitates T6P to trehalose conversion by trehalose-6-
744 P phosphatase, thereby re-allocating resources from source to sink tissues likely through
745 SnRK1's phosphorylation and activation of C/S1 basic region-leucine zipper transcription
746 factors (Smeekens, 2015).
747

748 **4. Conclusions**

749 Phosphate availability is a critical determinant of plant growth and development,
750 influencing complex regulatory networks at molecular, cellular, and physiological levels.
751 Our study resolved Pi-induced spatiotemporal changes to the Arabidopsis shoot and root
752 proteomes, validating our current understanding and providing a number of novel insights
753 into the dynamic nature of the PSR. We observed distinct and overlapping regulatory
754 trends in shoots and roots at both early (1 h) and late (48 h) time-points. Classical PSR

755 proteins (e.g., PHTs, PAPs, metabolic bypass enzymes, phospholipases) were generally
756 downregulated following Pi resupply, although this downregulation varied between
757 tissues and time-points highlighting a finely tuned system for Pi redistribution during
758 recovery from Pi-starvation (Figure 5).

759 Overall, early responses predominantly involved metabolic adjustments to restore Pi
760 pools via enhanced glycolysis and energy production, while late responses were
761 characterized by metabolic shifts prioritizing anabolic processes including membrane
762 remodeling and nucleotide production. This was especially notable in shoots, where the
763 early upregulation of photosynthetic proteins at 1 h may reflect a transient need to restore
764 photosynthetic capacity, followed by downregulation at 48 h that could help mitigate the
765 risk of photoinhibition and ROS accumulation. Proteins involved in carbohydrate
766 metabolism (e.g., FBA5, PU1, G6PD1) demonstrated a similar early upregulation followed
767 by a delayed downregulation, reinforcing this trend. We also observed a dramatic
768 upregulation of ribosomal proteins (i.e. translation machinery) at 48 h, and a concurrent
769 downregulation of alternative splicing factors, some of which were implicated in plant
770 abiotic and nutritional stress responses. Collectively, our study provides a
771 comprehensive, proteome-centric framework of the plant PSR. These identifications, new
772 and previously established, not only enhance our current understanding of plant
773 nutritional stress responses but can also offer potential targets for biotechnological
774 interventions aimed at improving crop Pi- acquisition and -use efficiency.

775

776 **ACKNOWLEDGEMENTS**

777 Financial support was provided by research and equipment grants from the Natural
778 Sciences and Engineering Research Council of Canada (NSERC) to WCP and RGU an
779 NSERC CGS-D award to KHB, and a Canada Foundation for Innovation (CFI) award to
780 RGU. The authors are grateful to Jack Moore of the Alberta Proteomics and Mass
781 Spectrometry Facility for assistance with mass spectrometer operation and maintenance.

782

783 **AUTHOR CONTRIBUTIONS**

784 MAS, LEG, KHB, DM - investigation; MAS, LEG, RGU - formal analysis; MAS, LEG, WCP,
785 RGU - manuscript assembly and editing.

DATA AVAILABILITY

Mass spectrometry data have been deposited to the ProteomeExchange Consortium (http://proteomecentral.proteomexchange.org) *via* the PRoteomics IDEntification Database (PRIDE; https://www.ebi.ac.uk/pride/) partner repository with the data set identifier PXD062427.

CONFLICTS OF INTEREST

None to Declare

ORCID

Milena A. Smith: n/a
Lauren E. Grubb: 0000-0003-2651-2875
Kirsten H. Benidickson: 0009-0000-0247-7521
Devang Mehta: 0000-0002-8911-1174
William C. Plaxton: 0000-0002-8447-7249
R. Glen Uhrig: 0000-0003-2773-4381

REFERENCES

Angkawijaya, A.E. *et al.* (2019) 'Expression Profiles of 2 Phosphate Starvation-Inducible Phosphocholine/Phosphoethanolamine Phosphatases, PECP1 and PS2, in Arabidopsis', *Frontiers in Plant Science*, 10. Available at: https://doi.org/10.3389/fpls.2019.00662.

Arias, M.C. *et al.* (2014) 'From dusk till dawn: the Arabidopsis thaliana sugar starving responsive network', *Frontiers in Plant Science*, 5. Available at: https://doi.org/10.3389/fpls.2014.00482.

Ascencio-Ibáñez, J.T. *et al.* (2008) 'Global Analysis of Arabidopsis Gene Expression Uncovers a Complex Array of Changes Impacting Pathogen Response and Cell Cycle during Geminivirus Infection', *Plant Physiology*, 148(1), pp. 436–454. Available at: https://doi.org/10.1104/pp.108.121038.

Awai, K. *et al.* (2001) 'Two types of MGDG synthase genes, found widely in both 16:3 and 18:3 plants, differentially mediate galactolipid syntheses in photosynthetic and nonphotosynthetic tissues in Arabidopsis thaliana', *Proceedings of the National Academy of Sciences*, 98(19), pp. 10960–10965. Available at: https://doi.org/10.1073/pnas.181331498.

Ayadi, A. *et al.* (2015) 'Reducing the Genetic Redundancy of Arabidopsis PHOSPHATE TRANSPORTER1 Transporters to Study Phosphate Uptake and Signaling', *Plant Physiology*, 167(4), pp. 1511–1526. Available at: https://doi.org/10.1104/pp.114.252338.

Bariola, P.A. *et al.* (1994) 'The Arabidopsis ribonuclease gene RNS1 is tightly controlled in response to phosphate limitation', *The Plant Journal*, 6(5), pp. 673–685. Available at: https://doi.org/10.1046/j.1365-313X.1994.6050673.x.

Bariola, P.A., MacIntosh, G.C. and Green, P.J. (1999) 'Regulation of S-Like Ribonuclease Levels in Arabidopsis. Antisense Inhibition of RNS1 orRNS2 Elevates Anthocyanin Accumulation1', *Plant Physiology*, 119(1), pp. 331–342. Available at: https://doi.org/10.1104/pp.119.1.331.

Bayle, V. *et al.* (2011) 'Arabidopsis thaliana High-Affinity Phosphate Transporters Exhibit Multiple Levels of Posttranslational Regulation', *The Plant Cell*, 23(4), pp. 1523–1535. Available at: https://doi.org/10.1105/tpc.110.081067.

Benidickson, K.H. *et al.* (2023) 'Glutamate decarboxylase-1 is essential for efficient acclimation of Arabidopsis thaliana to nutritional phosphorus deprivation', *New Phytologist*, 240(6), pp. 2372–2385. Available at: https://doi.org/10.1111/nph.19300.

Binder, S., Knill, T. and Schuster, J. (2007) 'Branched-chain amino acid metabolism in higher plants', *Physiologia Plantarum*, 129(1), pp. 68–78. Available at: https://doi.org/10.1111/j.1399-3054.2006.00800.x.

Blackwell, M., Darch, T. and Haslam, R. (2019) 'Phosphorus use efficiency and fertilizers: future opportunities for improvements', *Frontiers of Agricultural Science and Engineering*, 6(4), pp. 332–340. Available at: https://doi.org/10.15302/J-FASE-2019274.

Bown, A.W. and Shelp, B.J. (2016) 'Plant GABA: Not Just a Metabolite', *Trends in Plant Science*, 21(10), pp. 811–813. Available at: https://doi.org/10.1016/j.tplants.2016.08.001.

842 Carstensen, A. *et al.* (2018) 'The Impacts of Phosphorus Deficiency on the Photosynthetic
843 Electron Transport Chain', *Plant Physiology*, 177(1), pp. 271–284. Available at:
844 https://doi.org/10.1104/pp.17.01624.

845 Chen, T. *et al.* (2013) 'A KH-Domain RNA-Binding Protein Interacts with FIERY2/CTD
846 Phosphatase-Like 1 and Splicing Factors and Is Important for Pre-mRNA Splicing in
847 Arabidopsis', *PLOS Genetics*, 9(10), p. e1003875. Available at:
848 https://doi.org/10.1371/journal.pgen.1003875.

849 Chen, W. *et al.* (2022) 'Research Advances in the Mutual Mechanisms Regulating Response of
850 Plant Roots to Phosphate Deficiency and Aluminum Toxicity', *International Journal of Molecular*
851 *Sciences*, 23(3), p. 1137. Available at: https://doi.org/10.3390/ijms23031137.

852 Chen, X. *et al.* (2019) 'Phosphatidylinositol-specific phospholipase C2 functions in auxin-
853 modulated root development', *Plant, Cell & Environment*, 42(5), pp. 1441–1457. Available at:
854 https://doi.org/10.1111/pce.13492.

855 Cheng, Y. *et al.* (2011) 'Characterization of the Arabidopsis glycerophosphodiester
856 phosphodiesterase (GDPD) family reveals a role of the plastid-localized AtGDPD1 in
857 maintaining cellular phosphate homeostasis under phosphate starvation', *The Plant Journal*,
858 66(5), pp. 781–795. Available at: https://doi.org/10.1111/j.1365-313X.2011.04538.x.

859 Choi, M.S. *et al.* (2005) 'Isolation of a Calmodulin-binding Transcription Factor from Rice (Oryza
860 sativa L.) *', *Journal of Biological Chemistry*, 280(49), pp. 40820–40831. Available at:
861 https://doi.org/10.1074/jbc.M504616200.

862 D'Ambrosio, J.M. *et al.* (2017) 'Phospholipase C2 Affects MAMP-Triggered Immunity by
863 Modulating ROS Production', *Plant Physiology*, 175(2), pp. 970–981. Available at:
864 https://doi.org/10.1104/pp.17.00173.

865 De Angeli, A. *et al.* (2013) 'AtALMT9 is a malate-activated vacuolar chloride channel required
866 for stomatal opening in Arabidopsis', *Nature Communications*, 4(1), p. 1804. Available at:
867 https://doi.org/10.1038/ncomms2815.

868 Del Pozo, J.C. *et al.* (1999) 'A type 5 acid phosphatase gene from Arabidopsis thaliana is
869 induced by phosphate starvation and by some other types of phosphate mobilising/oxidative
870 stress conditions', *The Plant Journal*, 19(5), pp. 579–589. Available at:
871 https://doi.org/10.1046/j.1365-313X.1999.00562.x.

872 Del Vecchio, H.A. *et al.* (2014) 'The cell wall-targeted purple acid phosphatase AtPAP25 is
873 critical for acclimation of Arabidopsis thaliana to nutritional phosphorus deprivation', *The Plant*
874 *Journal*, 80(4), pp. 569–581. Available at: https://doi.org/10.1111/tpj.12663.

875 Delatte, T. *et al.* (2006) 'Evidence for Distinct Mechanisms of Starch Granule Breakdown in
876 Plants*', *Journal of Biological Chemistry*, 281(17), pp. 12050–12059. Available at:
877 https://doi.org/10.1074/jbc.M513661200.

878 Dissanayaka, D.M.S.B. *et al.* (2021) 'Recent insights into the metabolic adaptations of
879 phosphorus-deprived plants', *Journal of Experimental Botany*, 72(2), pp. 199–223. Available at:
880 https://doi.org/10.1093/jxb/eraa482.

881 Doehlert, D.C. and Huber, S.C. (1984) 'Phosphate Inhibition of Spinach Leaf Sucrose
882 Phosphate Synthase as Affected by Glucose-6-Phosphate and Phosphoglucoisomerase 1',
883 *Plant Physiology*, 76(1), pp. 250–253. Available at: https://doi.org/10.1104/pp.76.1.250.

884 Dong, C. *et al.* (2018) 'Alternative Splicing Plays a Critical Role in Maintaining Mineral Nutrient
885 Homeostasis in Rice (Oryza sativa)', *The Plant Cell*, 30(10), pp. 2267–2285. Available at:
886 https://doi.org/10.1105/tpc.18.00051.

887 Duff, S.M.G., Moorhead, G.B.G., Lefebvre, D.D., and Plaxton, W.C.P. (1989) 'Phosphate
888 starvation inducible 'bypasses' of adenylate and phosphate dependent glycolytic enzymes in
889 *Brassica nigra* suspension cells', *Plant Physiology,* 90, pp.1275-1278. 10.1104/pp.90.4.1275.

890 Essigmann, B. *et al.* (1998) 'Phosphate availability affects the thylakoid lipid composition and
891 the expression of SQD1, a6, #ne required for sulfolipid biosynthesis in Arabidopsis thaliana',
892 *Proceedings of the National Academy of Sciences*, 95(4), pp. 1950–1955. Available at:
893 https://doi.org/10.1073/pnas.95.4.1950.

894 Feria, A.B. *et al.* (2016) 'Phosphoenolpyruvate carboxylase (PEPC) and PEPC-kinase (PEPC-k)
895 isoenzymes in Arabidopsis thaliana: role in control and abiotic stress conditions', *Planta*, 244(4),
896 pp. 901–913. Available at: https://doi.org/10.1007/s00425-016-2556-9.

897 Fujiki, Y. *et al.* (2005) 'Response to Darkness of Late-Responsive Dark-Inducible Genes is
898 Positively Regulated by Leaf Age and Negatively Regulated by Calmodulin-Antagonist-Sensitive
899 Signalling in Arabidopsis thaliana', *Plant and Cell Physiology*, 46(10), pp. 1741–1746. Available
900 at: https://doi.org/10.1093/pcp/pci174.

901 Gao, R. *et al.* (2023) 'Comprehensive study of serine/arginine-rich (SR) gene family in rice:
902 characterization, evolution and expression analysis', *PeerJ*, 11, p. e16193. Available at:
903 https://doi.org/10.7717/peerj.16193.

904 Georges, F. *et al.* (2009) 'Over-expression of Brassica napus phosphatidylinositol-
905 phospholipase C2 in canola induces significant changes in gene expression and phytohormone
906 distribution patterns, enhances drought tolerance and promotes early flowering and maturation',
907 *Plant, Cell & Environment*, 32(12), pp. 1664–1681. Available at: https://doi.org/10.1111/j.1365-
908 3040.2009.02027.x.

909 Ghahremani, M., Park, J., *et al.* (2019a) 'Lectin AtGAL1 interacts with high-mannose glycoform
910 of the purple acid phosphatase AtPAP26 secreted by phosphate-starved Arabidopsis', *Plant,*
911 *Cell & Environment*, 42(4), pp. 1158–1166. Available at: https://doi.org/10.1111/pce.13463.

912 Ghahremani, M., Tran, H., *et al.* (2019b) 'A glycoform of the secreted purple acid phosphatase
913 AtPAP26 co-purifies with a mannose-binding lectin (AtGAL1) upregulated by phosphate-starved
914 Arabidopsis', *Plant, Cell & Environment*, 42(4), pp. 1139–1157. Available at:
915 https://doi.org/10.1111/pce.13432.

916 Gho, Y.-S. *et al.* (2020) 'Phosphate-Starvation-Inducible S-Like RNase Genes in Rice Are
917 Involved in Phosphate Source Recycling by RNA Decay', *Frontiers in Plant Science*, 11.
918 Available at: https://doi.org/10.3389/fpls.2020.585561.

919 Gilliham, M. and Tyerman, S.D. (2016) 'Linking Metabolism to Membrane Signaling: The
920 GABA–Malate Connection', *Trends in Plant Science*, 21(4), pp. 295–301. Available at:
921 https://doi.org/10.1016/j.tplants.2015.11.011.

922 Gilliham, M. and Xu, B. (2022) 'γ-Aminobutyric acid may directly or indirectly regulate
923 Arabidopsis ALMT9', *Plant Physiology*, 190(3), pp. 1570–1573. Available at:
924 https://doi.org/10.1093/plphys/kiac399.

925 Gregory, A.L. *et al.* (2009) 'In vivo regulatory phosphorylation of the phosphoenolpyruvate
926 carboxylase AtPPC1 in phosphate-starved Arabidopsis thaliana', *Biochemical Journal*, 420(1),
927 pp. 57–65. Available at: https://doi.org/10.1042/BJ20082397.

928 Guo, M. *et al.* (2022) 'Alternative splicing of REGULATOR OF LEAF INCLINATION 1 modulates
929 phosphate starvation signaling and growth in plants', *The Plant Cell*, 34(9), pp. 3319–3338.
930 Available at: https://doi.org/10.1093/plcell/koac161.

931 Ham, B.-K. *et al.* (2018) 'Insights into plant phosphate sensing and signaling', *Current Opinion in*
932 *Biotechnology*, 49, pp. 1–9. Available at: https://doi.org/10.1016/j.copbio.2017.07.005.

933 Hammond, J.P. *et al.* (2003) 'Changes in Gene Expression in Arabidopsis Shoots during
934 Phosphate Starvation and the Potential for Developing Smart Plants', *Plant Physiology*, 132(2),
935 pp. 578–596. Available at: https://doi.org/10.1104/pp.103.020941.

936 Hammond, J.P. and White, P.J. (2008) 'Sucrose transport in the phloem: integrating root
937 responses to phosphorus starvation', *Journal of Experimental Botany*, 59(1), pp. 93–109.
938 Available at: https://doi.org/10.1093/jxb/erm221.

939 Hanchi, M. *et al.* (2018) 'The Phosphate Fast-Responsive Genes PECP1 and PPsPase1 Affect
940 Phosphocholine and Phosphoethanolamine Content', *Plant Physiology*, 176(4), pp. 2943–2962.
941 Available at: https://doi.org/10.1104/pp.17.01246.

942 Hinsinger, P. (2001) 'Bioavailability of soil inorganic P in the rhizosphere as affected by root-
943 induced chemical changes: a review', *Plant and Soil*, 237(2), pp. 173–195. Available at:
944 https://doi.org/10.1023/A:1013351617532.

945 van Hooren, M. *et al.* (2024) 'Ectopic Expression of Distinct PLC Genes Identifies
946 "Compactness" as a Possible Architectural Shoot Strategy to Cope with Drought Stress', *Plant*
947 *and Cell Physiology*, 65(6), pp. 885–903. Available at: https://doi.org/10.1093/pcp/pcad123.

948 Hurley, B.A. *et al.* (2010) 'The Dual-Targeted Purple Acid Phosphatase Isozyme AtPAP26 Is
949 Essential for Efficient Acclimation of Arabidopsis to Nutritional Phosphate Deprivation', *Plant*
950 *Physiology*, 153(3), pp. 1112–1122. Available at: https://doi.org/10.1104/pp.110.153270.

951 Iida, K. and Go, M. (2006) 'Survey of Conserved Alternative Splicing Events of mRNAs
952 Encoding SR Proteins in Land Plants', *Molecular Biology and Evolution*, 23(5), pp. 1085–1094.
953 Available at: https://doi.org/10.1093/molbev/msj118.

954 Jaślan, J. and De Angeli, A. (2022) 'Heterologous expression reveals that GABA does not
955 directly inhibit the vacuolar anion channel AtALMT9', *Plant Physiology*, 189(2), pp. 469–472.
956 Available at: https://doi.org/10.1093/plphys/kiac132.

Jung, J.-Y. *et al.* (2018) ‘Control of plant phosphate homeostasis by inositol pyrophosphates and the SPX domain’, *Current Opinion in Biotechnology*, 49, pp. 156–162. Available at: https://doi.org/10.1016/j.copbio.2017.08.012.

Karlsson, P.M. *et al.* (2015) ‘The Arabidopsis thylakoid transporter PHT4;1 influences phosphate availability for ATP synthesis and plant growth’, *The Plant Journal*, 84(1), pp. 99–110. Available at: https://doi.org/10.1111/tpj.12962.

Khan, G.A. *et al.* (2014) ‘Coordination between zinc and phosphate homeostasis involves the transcription factor PHR1, the phosphate exporter PHO1, and its homologue PHO1;H3 in Arabidopsis’, *Journal of Experimental Botany*, 65(3), pp. 871–884. Available at: https://doi.org/10.1093/jxb/ert444.

Kim, S.Y. *et al.* (2019) ‘In vivo evidence for a regulatory role of phosphorylation of Arabidopsis Rubisco activase at the Thr78 site’, *Proceedings of the National Academy of Sciences*, 116(37), pp. 18723–18731. Available at: https://doi.org/10.1073/pnas.1812916116.

Kobayashi, K. *et al.* (2009) ‘Type-B monogalactosyldiacylglycerol synthases are involved in phosphate starvation-induced lipid remodeling, and are crucial for low-phosphate adaptation’, *The Plant Journal*, 57(2), pp. 322–331. Available at: https://doi.org/10.1111/j.1365-313X.2008.03692.x.

Kobayashi, Yasufumi *et al.* (2013) ‘Molecular and Physiological Analysis of Al3+ and H+ Rhizotoxicities at Moderately Acidic Conditions’, *Plant Physiology*, 163(1), pp. 180–192. Available at: https://doi.org/10.1104/pp.113.222893.

Köck, M. *et al.* (1998) ‘Extracellular administration of phosphate-sequestering metabolites induces ribonucleases in cultured tomato cells’, *Planta*, 204(3), pp. 404–407. Available at: https://doi.org/10.1007/s004250050273.

Lambers, H. and Plaxton, W.C. (2015) ‘Phosphorus: Back to the Roots’, in *Annual Plant Reviews Volume 48*. John Wiley & Sons, Ltd, pp. 1–22. Available at: https://doi.org/10.1002/9781118958841.ch1.

Lei, M. *et al.* (2011) ‘Genetic and Genomic Evidence That Sucrose Is a Global Regulator of Plant Responses to Phosphate Starvation in Arabidopsis’, *Plant Physiology*, 156(3), pp. 1116–1130. Available at: https://doi.org/10.1104/pp.110.171736.

Leutert, M. *et al.* (2019) ‘R2-P2 rapid-robotic phosphoproteomics enables multidimensional cell signaling studies’, *Molecular Systems Biology*, 15(12), p. e9021. Available at: https://doi.org/10.15252/msb.20199021.

Li, H. *et al.* (2023) ‘Molecular mechanism of phosphorous signaling inducing anthocyanin accumulation in *Arabidopsis*’, *Plant Physiology and Biochemistry*, 196, pp. 121–129. Available at: https://doi.org/10.1016/j.plaphy.2023.01.029.

Li, S. *et al.* (2016) ‘MYB75 Phosphorylation by MPK4 Is Required for Light-Induced Anthocyanin Accumulation in Arabidopsis’, *The Plant Cell*, 28(11), pp. 2866–2883. Available at: https://doi.org/10.1105/tpc.16.00130.

995 Liang, L. *et al.* (2002) '*AhSL28*, a senescence- and phosphate starvation-induced S-like RNase
996 gene in *Antirrhinum*', *Biochimica et Biophysica Acta (BBA) - Gene Structure and Expression*,
997 1579(1), pp. 64–71. Available at: https://doi.org/10.1016/S0167-4781(02)00507-9.

998 Liu, C. *et al.* (2020) 'Arabidopsis *mgd* mutants with reduced monogalactosyldiacylglycerol
999 contents are hypersensitive to aluminium stress', *Ecotoxicology and Environmental Safety*, 203,
1000 p. 110999. Available at: https://doi.org/10.1016/j.ecoenv.2020.110999.

1001 Liu, T.-Y. *et al.* (2016) 'Identification of plant vacuolar transporters mediating phosphate
1002 storage', *Nature Communications*, 7(1), p. 11095. Available at:
1003 https://doi.org/10.1038/ncomms11095.

1004 Liu, Z. *et al.* (2022) 'PHR1 positively regulates phosphate starvation-induced anthocyanin
1005 accumulation through direct upregulation of genes F3'H and LDOX in Arabidopsis', *Planta*,
1006 256(2), p. 42. Available at: https://doi.org/10.1007/s00425-022-03952-w.

1007 Liu, A.Y. *et al.* (2025_ 'Vacuolar phosphatases are essential for efficient nucleotide salvage in
1008 Arabidopsis', *Journal of Experimental Botany*, eraf168, https:// doi.org/10.1093/jxb/eraf168

1009 Luo, X. *et al.* (2021) 'Phosphate deficiency enhances cotton resistance to *Verticillium dahliae*
1010 through activating jasmonic acid biosynthesis and phenylpropanoid pathway', *Plant Science*,
1011 302, p. 110724. Available at: https://doi.org/10.1016/j.plantsci.2020.110724.

1012 Mangeon, A. *et al.* (2016) 'AtGRP3 Is Implicated in Root Size and Aluminum Response
1013 Pathways in Arabidopsis', *PLOS ONE*, 11(3), p. e0150583. Available at:
1014 https://doi.org/10.1371/journal.pone.0150583.

1015 Maruyama, H. *et al.* (2019) 'AtALMT3 is Involved in Malate Efflux Induced by Phosphorus
1016 Deficiency in Arabidopsis thaliana Root Hairs', *Plant and Cell Physiology*, 60(1), pp. 107–115.
1017 Available at: https://doi.org/10.1093/pcp/pcy190.

1018 Masakapalli, S.K. *et al.* (2014) 'The metabolic flux phenotype of heterotrophic Arabidopsis cells
1019 reveals a flexible balance between the cytosolic and plastidic contributions to carbohydrate
1020 oxidation in response to phosphate limitation', *The Plant Journal*, 78(6), pp. 964–977. Available
1021 at: https://doi.org/10.1111/tpj.12522.

1022 Mehta, D. *et al.* (2021) 'Phosphate and phosphite have a differential impact on the proteome
1023 and phosphoproteome of Arabidopsis suspension cell cultures', *The Plant Journal*, 105(4), pp.
1024 924–941. Available at: https://doi.org/10.1111/tpj.15078.

1025 Mehta, D., Scandola, S. and Uhrig, R.G. (2022) 'BoxCar and Library-Free Data-Independent
1026 Acquisition Substantially Improve the Depth, Range, and Completeness of Label-Free
1027 Quantitative Proteomics', *Analytical Chemistry*, 94(2), pp. 793–802. Available at:
1028 https://doi.org/10.1021/acs.analchem.1c03338.

1029 Misson, J. *et al.* (2005) 'A genome-wide transcriptional analysis using Arabidopsis thaliana
1030 Affymetrix gene chips determined plant responses to phosphate deprivation', *Proceedings of the*
1031 *National Academy of Sciences*, 102(33), pp. 11934–11939. Available at:
1032 https://doi.org/10.1073/pnas.0505266102.

1033 van de Mortel, J.E. *et al.* (2006) 'Large Expression Differences in Genes for Iron and Zinc
1034 Homeostasis, Stress Response, and Lignin Biosynthesis Distinguish Roots of Arabidopsis
1035 thaliana and the Related Metal Hyperaccumulator Thlaspi caerulescens', *Plant Physiology*,
1036 142(3), pp. 1127–1147. Available at: https://doi.org/10.1104/pp.106.082073.

1037 Müller, R. *et al.* (2004) 'Gene expression during recovery from phosphate starvation in roots and
1038 shoots of Arabidopsis thaliana', *Physiologia Plantarum*, 122(2), pp. 233–243. Available at:
1039 https://doi.org/10.1111/j.1399-3054.2004.00394.x.

1040 Nakamura, Y. *et al.* (2005) 'A Novel Phosphatidylcholine-hydrolyzing Phospholipase C Induced
1041 by Phosphate Starvation in *Arabidopsis**', *Journal of Biological Chemistry*, 280(9), pp. 7469–
1042 7476. Available at: https://doi.org/10.1074/jbc.M408799200.

1043 Nakamura, Y. *et al.* (2009) 'Arabidopsis lipins mediate eukaryotic pathway of lipid metabolism
1044 and cope critically with phosphate starvation', *Proceedings of the National Academy of*
1045 *Sciences*, 106(49), pp. 20978–20983. Available at: https://doi.org/10.1073/pnas.0907173106.

1046 Nitenberg, M. *et al.* (2020) 'Mechanism of activation of plant monogalactosyldiacylglycerol
1047 synthase 1 (MGD1) by phosphatidylglycerol', *Glycobiology*, 30(6), pp. 396–406. Available at:
1048 https://doi.org/10.1093/glycob/cwz106.

1049 O'Gallagher, B. *et al.* (2022) 'Arabidopsis PAP17 is a dual-localized purple acid phosphatase
1050 up-regulated during phosphate deprivation, senescence, and oxidative stress', *Journal of*
1051 *Experimental Botany*, 73(1), pp. 382–399. Available at: https://doi.org/10.1093/jxb/erab409.

1052 Okazaki, Y. *et al.* (2009) 'A Chloroplastic UDP-Glucose Pyrophosphorylase from Arabidopsis Is
1053 the Committed Enzyme for the First Step of Sulfolipid Biosynthesis', *The Plant Cell*, 21(3), pp.
1054 892–909. Available at: https://doi.org/10.1105/tpc.108.063925.

1055 Oropeza-Aburto, A. *et al.* (2012) 'Functional analysis of the Arabidopsis PLDZ2 promoter
1056 reveals an evolutionarily conserved low-Pi-responsive transcriptional enhancer element',
1057 *Journal of Experimental Botany*, 63(5), pp. 2189–2202. Available at:
1058 https://doi.org/10.1093/jxb/err446.

1059 Palma, D.A., Blumwald, E. and Plaxton, W.C. (2000) 'Upregulation of vacuolar H+-translocating
1060 pyrophosphatase by phosphate starvation of Brassica napus (rapeseed) suspension cell
1061 cultures', *FEBS Letters*, 486(2), pp. 155–158. Available at: https://doi.org/10.1016/S0014-
1062 5793(00)02266-3.

1063 Panda, S.K., Baluška ,František and and Matsumoto, H. (2009) 'Aluminum stress signaling in
1064 plants', *Plant Signaling & Behavior*, 4(7), pp. 592–597. Available at:
1065 https://doi.org/10.4161/psb.4.7.8903.

1066 Parsons, H.L., Yip, J.Y.H. and Vanlerberghe, G.C. (1999) 'Increased Respiratory Restriction
1067 during Phosphate-Limited Growth in Transgenic Tobacco Cells Lacking Alternative Oxidase1',
1068 *Plant Physiology*, 121(4), pp. 1309–1320. Available at: https://doi.org/10.1104/pp.121.4.1309.

1069 Ramaiah, M. *et al.* (2011) 'Characterization of the Phosphate Starvation-Induced Glycerol-3-
1070 phosphate permease Gene Family in Arabidopsis', *Plant Physiology*, 157(1), pp. 279–291.
1071 Available at: https://doi.org/10.1104/pp.111.178541.

1072 Ramesh, S.A. *et al.* (2015) 'GABA signalling modulates plant growth by directly regulating the
1073 activity of plant-specific anion transporters', *Nature Communications*, 6(1), p. 7879. Available at:
1074 https://doi.org/10.1038/ncomms8879.

1075 Robinson, W.D., Carson, I., *et al.* (2012a) 'Eliminating the purple acid phosphatase AtPAP26 in
1076 Arabidopsis thaliana delays leaf senescence and impairs phosphorus remobilization', *New*
1077 *Phytologist*, 196(4), pp. 1024–1029. Available at: https://doi.org/10.1111/nph.12006.

1078 Robinson, W.D., Park, J., *et al.* (2012b) 'The secreted purple acid phosphatase isozymes
1079 AtPAP12 and AtPAP26 play a pivotal role in extracellular phosphate-scavenging by Arabidopsis
1080 thaliana', *Journal of Experimental Botany*, 63(18), pp. 6531–6542. Available at:
1081 https://doi.org/10.1093/jxb/ers309.

1082 Rojas, B.E. and Iglesias, A.A. (2023) 'Integrating multiple regulations on enzyme activity: the
1083 case of phosphoenolpyruvate carboxykinases', *AoB PLANTS*, 15(4), p. plad053. Available at:
1084 https://doi.org/10.1093/aobpla/plad053.

1085 Rojas, H.J., Roldán, J.A. and Goldraij, A. (2013) 'NnSR1, a class III non-S-RNase constitutively
1086 expressed in styles, is induced in roots and stems under phosphate deficiency in Nicotiana
1087 alata', *Annals of Botany*, 112(7), pp. 1351–1360. Available at:
1088 https://doi.org/10.1093/aob/mct207.

1089 Schluepmann, H. *et al.* (2004) 'Trehalose Mediated Growth Inhibition of Arabidopsis Seedlings
1090 Is Due to Trehalose-6-Phosphate Accumulation', *Plant Physiology*, 135(2), pp. 879–890.
1091 Available at: https://doi.org/10.1104/pp.104.039503.

1092 Sivaguru, M. *et al.* (2003) 'Aluminum-Induced Gene Expression and Protein Localization of a
1093 Cell Wall-Associated Receptor Kinase in Arabidopsis', *Plant Physiology*, 132(4), pp. 2256–2266.
1094 Available at: https://doi.org/10.1104/pp.103.022129.

1095 Smeekens, S. (2015) 'From Leaf to Kernel: Trehalose-6-Phosphate Signaling Moves Carbon in
1096 the Field', *Plant Physiology*, 169(2), pp. 912–913. Available at:
1097 https://doi.org/10.1104/pp.15.01177.

1098 Smith, M.A., Benidickson, K.H. and Plaxton, W.C. (2024) 'In Vivo Phosphorylation of the
1099 Cytosolic Glucose-6-Phosphate Dehydrogenase Isozyme G6PD6 in Phosphate-Resupplied
1100 Arabidopsis thaliana Suspension Cells and Seedlings', *Plants*, 13(1), p. 31. Available at:
1101 https://doi.org/10.3390/plants13010031.

1102 Stefanovic, A. *et al.* (2011) 'Over-expression of PHO1 in Arabidopsis leaves reveals its role in
1103 mediating phosphate efflux', *The Plant Journal*, 66(4), pp. 689–699. Available at:
1104 https://doi.org/10.1111/j.1365-313X.2011.04532.x.

1105 Stigter, K.A. and Plaxton, W.C. (2015) 'Molecular Mechanisms of Phosphorus Metabolism and
1106 Transport during Leaf Senescence', *Plants*, 4(4), pp. 773–798. Available at:
1107 https://doi.org/10.3390/plants4040773.

1108 Su, Y. *et al.* (2018) 'Different effects of phospholipase Dζ2 and non-specific phospholipase C4
1109 on lipid remodeling and root hair growth in Arabidopsis response to phosphate deficiency', *The*
1110 *Plant Journal*, 94(2), pp. 315–326. Available at: https://doi.org/10.1111/tpj.13858.

1111 Symonds, K. *et al.* (2024) 'Characterization of Arabidopsis aldolases AtFBA4, AtFBA5, and their
1112 inhibition by morin and interaction with calmodulin', *FEBS Letters*, 598(15), pp. 1864–1876.
1113 Available at: https://doi.org/10.1002/1873-3468.14979.

1114 Tannert, M. *et al.* (2018) 'Pi starvation-dependent regulation of ethanolamine metabolism by
1115 phosphoethanolamine phosphatase PECP1 in Arabidopsis roots', *Journal of Experimental*
1116 *Botany*, 69(3), pp. 467–481. Available at: https://doi.org/10.1093/jxb/erx408.

1117 Tao, H. *et al.* (2024) 'WRKY33 negatively regulates anthocyanin biosynthesis and cooperates
1118 with PHR1 to mediate acclimation to phosphate starvation', *Plant Communications*, 5(5), p.
1119 100821. Available at: https://doi.org/10.1016/j.xplc.2024.100821.

1120 Taylor, C.B. *et al.* (1993) 'RNS2: a senescence-associated RNase of Arabidopsis that diverged
1121 from the S-RNases before speciation.', *Proceedings of the National Academy of Sciences*,
1122 90(11), pp. 5118–5122. Available at: https://doi.org/10.1073/pnas.90.11.5118.

1123 Theodorou, M.E. and Plaxton, W.C. (1994) 'Induction of PPi-dependent phosphofructokinase by
1124 phosphate starvation in seedlings of Brassica nigra', *Plant, Cell & Environment*, 17(3), pp. 287–
1125 294. Available at: https://doi.org/10.1111/j.1365-3040.1994.tb00294.x.

1126 Ticconi, C.A. *et al.* (2009) 'ER-resident proteins PDR2 and LPR1 mediate the developmental
1127 response of root meristems to phosphate availability', *Proceedings of the National Academy of*
1128 *Sciences*, 106(33), pp. 14174–14179. Available at: https://doi.org/10.1073/pnas.0901778106.

1129 Tran, H.T. *et al.* (2010) 'Biochemical and molecular characterization of AtPAP12 and AtPAP26:
1130 the predominant purple acid phosphatase isozymes secreted by phosphate-starved Arabidopsis
1131 thaliana', *Plant, Cell & Environment*, 33(11), pp. 1789–1803. Available at:
1132 https://doi.org/10.1111/j.1365-3040.2010.02184.x.

1133 Tran, H.T., Hurley, B.A. and Plaxton, W.C. (2010) 'Feeding hungry plants: The role of purple
1134 acid phosphatases in phosphate nutrition', *Plant Science*, 179(1), pp. 14–27. Available at:
1135 https://doi.org/10.1016/j.plantsci.2010.04.005.

1136 Veljanovski, V. *et al.* (2006) 'Biochemical and Molecular Characterization of AtPAP26, a
1137 Vacuolar Purple Acid Phosphatase Up-Regulated in Phosphate-Deprived Arabidopsis
1138 Suspension Cells and Seedlings', *Plant Physiology*, 142(3), pp. 1282–1293. Available at:
1139 https://doi.org/10.1104/pp.106.087171.

1140 Veneklaas, E.J. *et al.* (2012) 'Opportunities for improving phosphorus-use efficiency in crop
1141 plants', *New Phytologist*, 195(2), pp. 306–320. Available at: https://doi.org/10.1111/j.1469-
1142 8137.2012.04190.x.

1143 Vijayraghavan, V. and Soole, K. (2010) 'Effect of short- and long-term phosphate stress on the
1144 non-phosphorylating pathway of mitochondrial electron transport in Arabidopsis thaliana',
1145 *Functional Plant Biology*, 37(5), pp. 455–466. Available at: https://doi.org/10.1071/FP09206.

1146 Wang, L. *et al.* (2011) 'The Arabidopsis Purple Acid Phosphatase AtPAP10 Is Predominantly
1147 Associated with the Root Surface and Plays an Important Role in Plant Tolerance to Phosphate
1148 Limitation', *Plant Physiology*, 157(3), pp. 1283–1299. Available at:
1149 https://doi.org/10.1104/pp.111.183723.

1150 Wang, L. *et al.* (2014) 'Comparative genetic analysis of Arabidopsis purple acid phosphatases
1151 AtPAP10, AtPAP12, and AtPAP26 provides new insights into their roles in plant adaptation to
1152 phosphate deprivation', *Journal of Integrative Plant Biology*, 56(3), pp. 299–314. Available at:
1153 https://doi.org/10.1111/jipb.12184.

1154 Wang, Yan *et al.* (2021) 'Phosphate Uptake and Transport in Plants: An Elaborate Regulatory
1155 System', *Plant and Cell Physiology*, 62(4), pp. 564–572. Available at:
1156 https://doi.org/10.1093/pcp/pcab011.

1157 Wang, Yanting *et al.* (2021) 'The role of strigolactones in P deficiency induced transcriptional
1158 changes in tomato roots', *BMC Plant Biology*, 21(1), p. 349. Available at:
1159 https://doi.org/10.1186/s12870-021-03124-0.

1160 Wang, Y.-H., Garvin, D.F. and Kochian, L.V. (2002) 'Rapid Induction of Regulatory and
1161 Transporter Genes in Response to Phosphorus, Potassium, and Iron Deficiencies in Tomato
1162 Roots. Evidence for Cross Talk and Root/Rhizosphere-Mediated Signals', *Plant Physiology*,
1163 130(3), pp. 1361–1370. Available at: https://doi.org/10.1104/pp.008854.

1164 Wu, P. *et al.* (2003) 'Phosphate Starvation Triggers Distinct Alterations of Genome Expression
1165 in Arabidopsis Roots and Leaves', *Plant Physiology*, 132(3), pp. 1260–1271. Available at:
1166 https://doi.org/10.1104/pp.103.021022.

1167 Xu, B. *et al.* (2021) 'GABA signalling modulates stomatal opening to enhance plant water use
1168 efficiency and drought resilience', *Nature Communications*, 12(1), p. 1952. Available at:
1169 https://doi.org/10.1038/s41467-021-21694-3.

1170 Yang, B. *et al.* (2021) 'Acylation of non-specific phospholipase C4 determines its function in
1171 plant response to phosphate deficiency', *The Plant Journal*, 106(6), pp. 1647–1659. Available
1172 at: https://doi.org/10.1111/tpj.15260.

1173 Yin, Y. and Ashihar, H. (2008) 'Expression of Glucose-6-phosphate Dehydrogenase and 6-
1174 Phosphogluconate Dehydrogenase Isoform Genes in Suspension-Cultured Arabidopsis thaliana
1175 Cells', *Zeitschrift für Naturforschung C*, 63(9–10), pp. 713–720. Available at:
1176 https://doi.org/10.1515/znc-2008-9-1017.

1177 Yoshitake, Y. *et al.* (2017) 'Arabidopsis Phosphatidic Acid Phosphohydrolases Are Essential for
1178 Growth under Nitrogen-Depleted Conditions', *Frontiers in Plant Science*, 8. Available at:
1179 https://doi.org/10.3389/fpls.2017.01847.

1180 Yu, B., Xu, C. and Benning, C. (2002) 'Arabidopsis disrupted in SQD2 encoding sulfolipid
1181 synthase is impaired in phosphate-limited growth', *Proceedings of the National Academy of*
1182 *Sciences*, 99(8), pp. 5732–5737. Available at: https://doi.org/10.1073/pnas.082696499.

1183 Zhang, W. *et al.* (2014) 'Splicing factor SR34b mutation reduces cadmium tolerance in
1184 *Arabidopsis* by regulating iron-regulated transporter 1 gene', *Biochemical and Biophysical*
1185 *Research Communications*, 455(3), pp. 312–317. Available at:
1186 https://doi.org/10.1016/j.bbrc.2014.11.017.

1187 Zhang, Y. *et al.* (2014) 'A major root-associated acid phosphatase in Arabidopsis, AtPAP10, is
1188 regulated by both local and systemic signals under phosphate starvation', *Journal of*
1189 *Experimental Botany*, 65(22), pp. 6577–6588. Available at: https://doi.org/10.1093/jxb/eru377.

1190 Zhou, M. *et al.* (2022) 'Proteomic Analysis Dissects Molecular Mechanisms Underlying Plant
1191 Responses to Phosphorus Deficiency', *Cells*, 11(4), p. 651. Available at:
1192 https://doi.org/10.3390/cells11040651.

1193

1194

1195 **SUPPORTING INFORMATION**

1196

1197 **Table S1.** All proteomics data for the manuscript. This includes: All quantified proteins,
1198 significantly changing proteins and Spectronaut v17 search parameter details.

1199

1200 **Table S2.** Enriched metabolic pathway analysis (PMN;
1201 https://www.plantcyc.org/databases/aracyc/8.0) using significantly changing proteins in
1202 shoots and roots following 1 and 48 h of Pi resupply.

1203

1204 **Table S3.** Differentially expressed significantly changing proteins

1205

1206 **Figure S1.** Subcellular localization of significantly changing proteins in Pi-resupplied
1207 *Arabidopsis* shoots and roots. *In silico* subcellular localization analysis of the significantly
1208 changing proteins that were down- or upregulated was performed using SUBAcon
1209 (https://suba.live/) for shoots and roots following 1 and 48 h of Pi resupply.

1210

1211 **Figure S2.** Summary of Pi responsive proteome. Heatmap of Pi-responsive proteome
1212 changes at 1 and 48 h after Pi resupply in shoots and roots relating to: (a) Pi sensing and
1213 transport, (b) membrane lipid remodeling, (c) Pi scavenging, and (d) and metabolic
1214 'bypass' enzymes. Scale represents the Log2FC at the specified timepoint following Pi
1215 resupply where blue indicates downregulated and yellow indicates upregulated proteins.

1216

1217 **FIGURE AND TABLE LEGENDS**

1218 **Table 1.** Established Pi starvation response proteins that were detected in our study.

1219 **Table 2.** Number of identified, quantified and significantly changing proteins.

1220

1221 **FIGURE 1** Sample preparation and validation. (a) Experimental workflow for preparation
1222 of 1 and 48 h Pi-starved (-Pi) and 2 mM Pi refed Arabidopsis seedlings. Images are
1223 examples of the -Pi and Pi-resupplied plants. (b) Seedling dry weight after 1 and 48h of
1224 Pi resupply represent means ±SE of n = 6 independent biological replicates. Significant
1225 differences were determined using the Student's t-test (** P-value <0.05). Specific APase
1226 activities of the clarified protein extracts from (c) shoots and (d) roots after 1 and 48 h of
1227 Pi resupply represent means ±SE of *n* = 3 independent determinations using samples
1228 prepared from 3 biological replicates. Significant differences were determined using the
1229 Student's t-test (***P-value < 0.05; ****P-value < 0.01).

1230

1231 **FIGURE 2** Distribution of significant shoot versus root proteome following Pi resupply of
1232 Arabidopsis seedlings. (a, b) Significantly changing shoot and root proteome (*q*-value <
1233 0.05; *n* = 4; -0.58 > Log_2 fold change (FC) > +0.58) in response to (a) 1 h or (b) 48 h of Pi
1234 resupply. Numbers denote the volume of significantly changed species on each axis or
1235 quadrant. Labeled proteins represent those with notable Log_2FC in total abundance. (c)
1236 Venn diagrams depicting the overlap of significantly changing proteins common between
1237 or independent of 1 and 48 h of Pi resupply (*q*-value < 0.05; *n* = 4).

1238

1239 **FIGURE 3** Gene Ontology (GO) enrichment analysis of shoot and root proteins increasing
1240 or decreasing upon Pi resupply. Dotplot representation of enriched biological process GO
1241 terms for significantly changing proteins (*q*-value <0.05; Log_2FC>0.58 or <0.58) that are
1242 up- or down-regulated in (a) shoots or (b) roots following 1 or 48 h of Pi resupply. The dot
1243 size indicates the gene ratio (number of proteins seen under the condition/total quantified
1244 proteins in this study). The colour code of the dots represents log10 (*p*-value) on a
1245 gradient from low to high or purple to yellow.

1246

1247 **FIGURE 4** Association network analysis of proteins whose abundance changed following
1248 1 and 48 h of Pi resupply. Association network analyses were performed using STRING-
1249 DB (ANOVA *p*-value <0.05) depicting significantly changing proteins following 1 and 48 h
1250 of Pi resupply in (a) shoots and (b) roots. Edge thickness indicates the strength of
1251 connection between nodes. Minimum edge threshold was set to 0.7 for roots and 0.9 for
1252 shoots. Node outer circles indicate the standardized relative Log2FC of the indicated
1253 protein in Pi resupply vs. -Pi. The scale of red to blue indicates relative increase and
1254 decrease in abundance, respectively. Grey circles encompass protein nodes involved in
1255 the same biological process.
1256
1257 **FIGURE 5** Summary of known proteomic changes observed following Pi refeeding in
1258 Arabidopsis shoots and roots. AOX, alternative oxidase; ETC, electron transport chain;
1259 GAD, glutamate decarboxylase; G6PD, glucose 6-P dehydrogenase; GDPD,
1260 glycerophosphodiester phosphodiesterase; MGD, monogalactosyldiacylglycerol
1261 synthase; NPC, non-specific phospholipase; OPPP, oxidative pentose phosphate
1262 pathway; PAH, phosphatidate phosphatase; PAP, purple acid phosphatase; 6PGL, 6-
1263 phosphogluconolactonase; PHT, Pi transporter; PL, phospholipase; PPC, plant type PEP
1264 carboxylase; RNS, ribonuclease; SDQ, sulfoquinovosyl diacylglycerol; TCA, tricarboxylic
1265 acid. Created in https://BioRender.com.

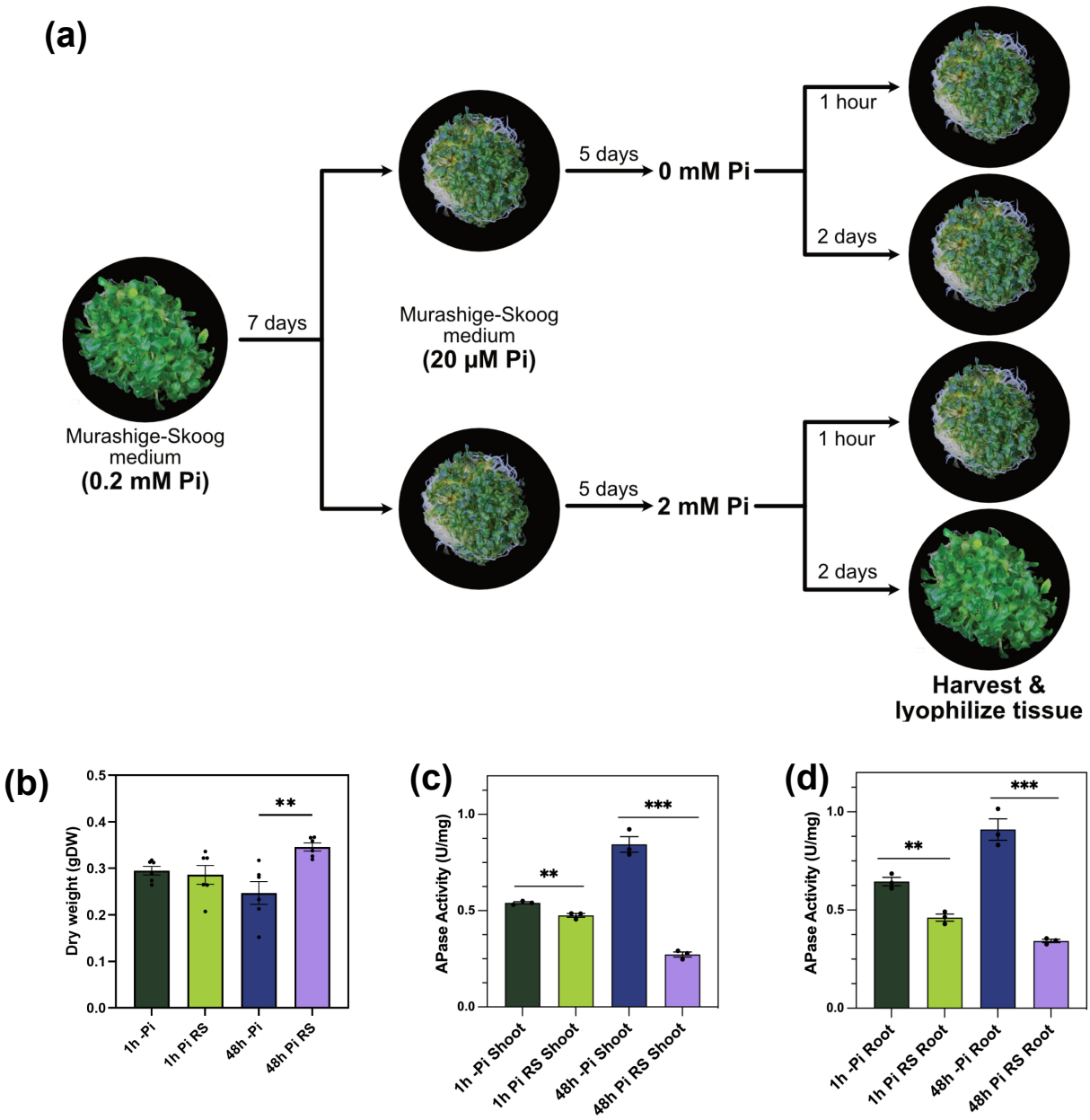

FIGURE 1 Sample preparation and validation. (a) Experimental workflow for preparation of 1 and 48 h Pi-starved (-Pi) and 2 mM Pi refed Arabidopsis seedlings. Images are examples of the -Pi and Pi-resupplied plants. Specific APase activities of the clarified protein extracts from (b) shoots and (c) roots after 1 and 48 h of Pi resupply represent means ±SE of *n* = 3 independent determinations using samples prepared from 3 biological replicates. Significant differences were determined using the Student's t-test (***P-value < 0.05; ****P-value < 0.01). (d) Seedling dry weight after 1 and 48 h of Pi resupply represent means ±SE of *n* = 6 independent biological replicates. Significant differences were determined using the Student's t-test (** P-value <0.05)

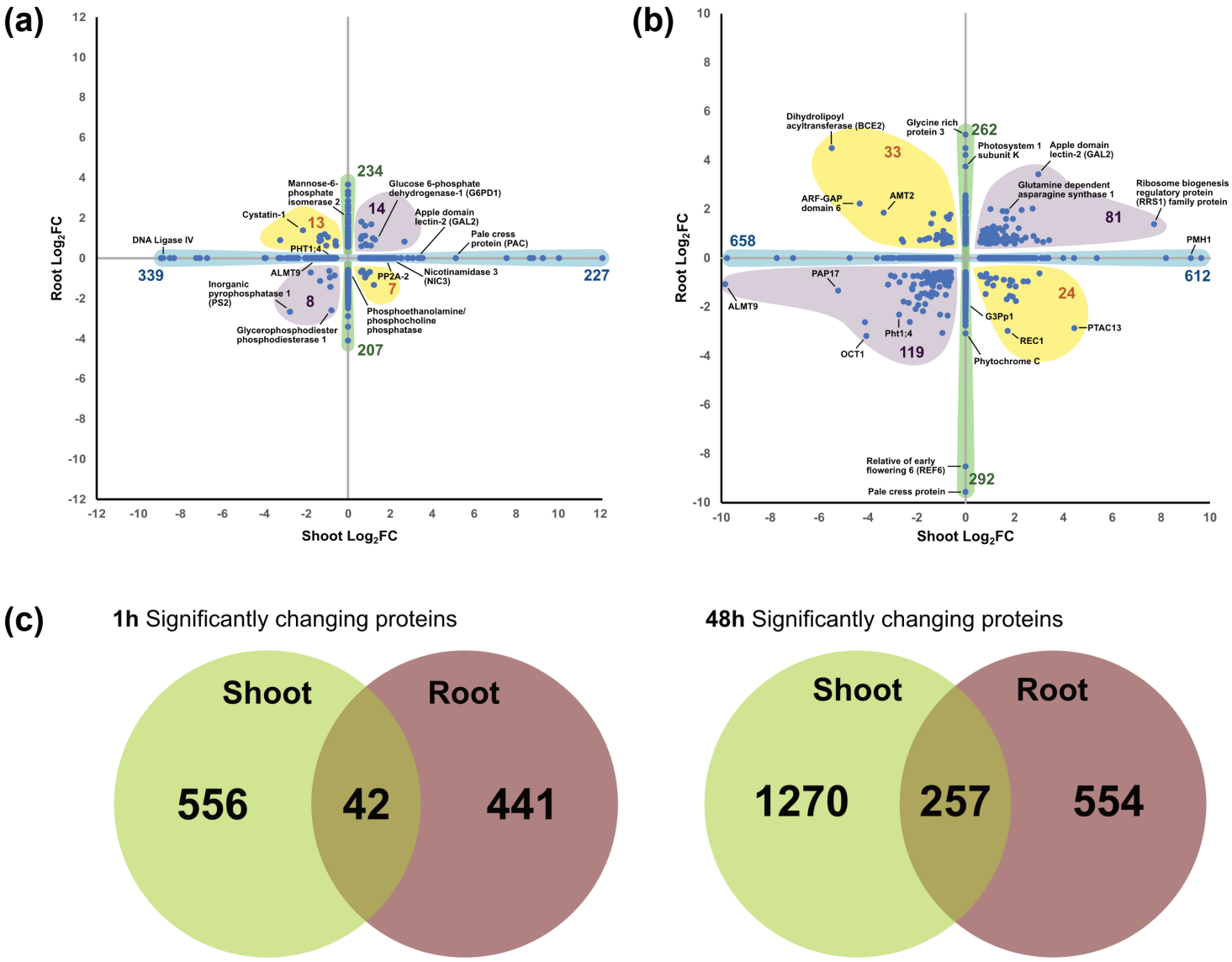

FIGURE 2 Distribution of significant shoot versus root proteome following Pi resupply of Arabidopsis seedlings. (a, b) Significantly changing shoot and root proteome (q-value < 0.05; n = 4; -0.58 > Log_2 fold change (FC) > +0.58) in response to (a) 1 h or (b) 48 h of Pi resupply. Numbers denote the volume of significantly changed species on each axis or quadrant. Labeled proteins represent those with notable Log_2FC in total abundance. (c) Venn diagrams depicting the overlap of significantly changing proteins common between or independent of 1 and 48 h of Pi resupply (q-value < 0.05; n = 4).

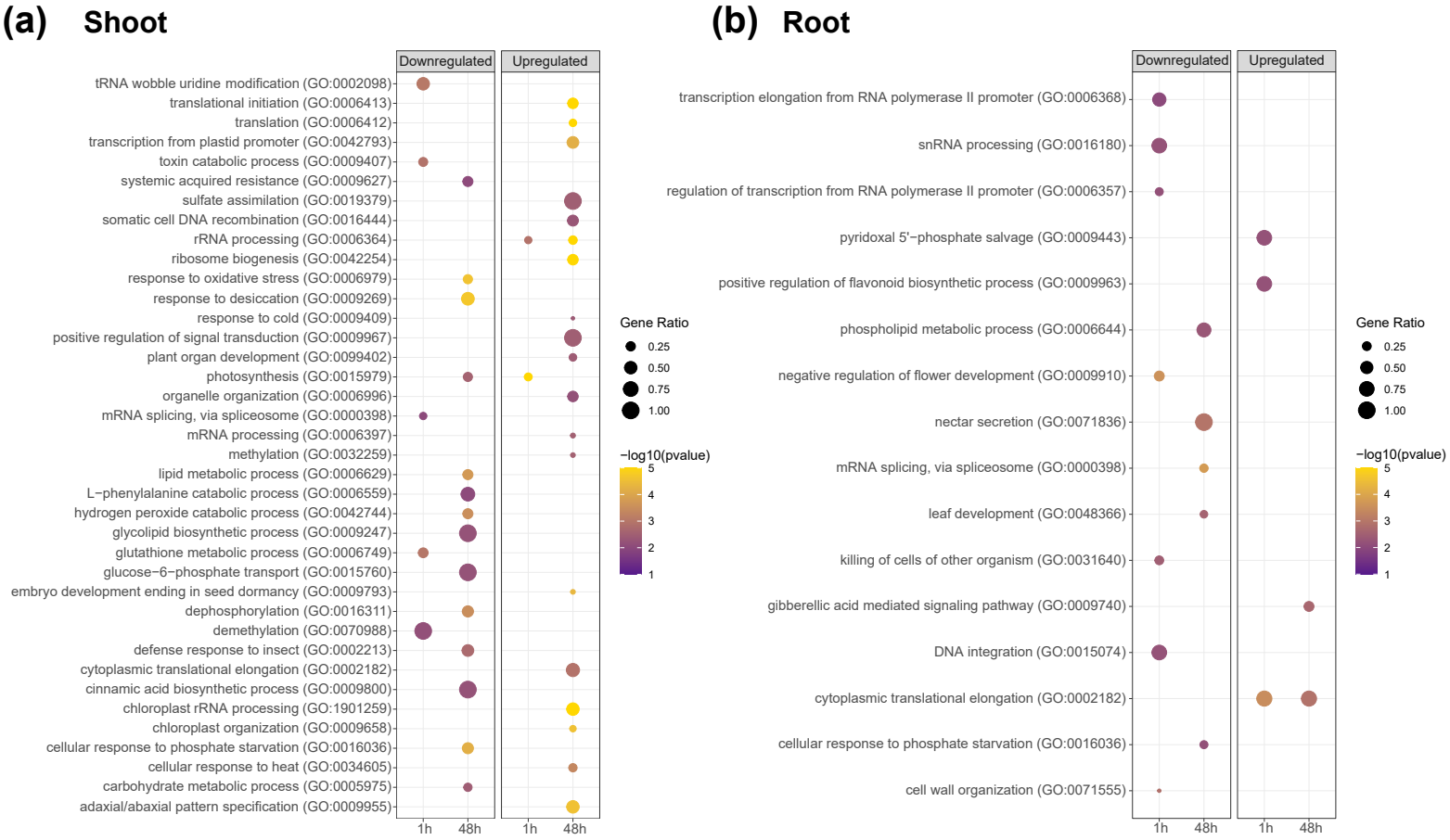

FIGURE 3 Gene Ontology (GO) enrichment analysis of shoot and root proteins increasing or decreasing upon Pi resupply. Dotplot representation of enriched biological process GO terms for significantly changing proteins (*q*-value <0.05; Log_2FC>0.58 or <0.58) that are up- or down-regulated in (a) shoots or (b) roots following 1 or 48 h of Pi resupply. The dot size indicates the gene ratio (number of proteins seen under the condition/total quantified proteins in this study). The colour code of the dots represents log10 (*p*-value) on a gradient from low to high or purple to yellow.

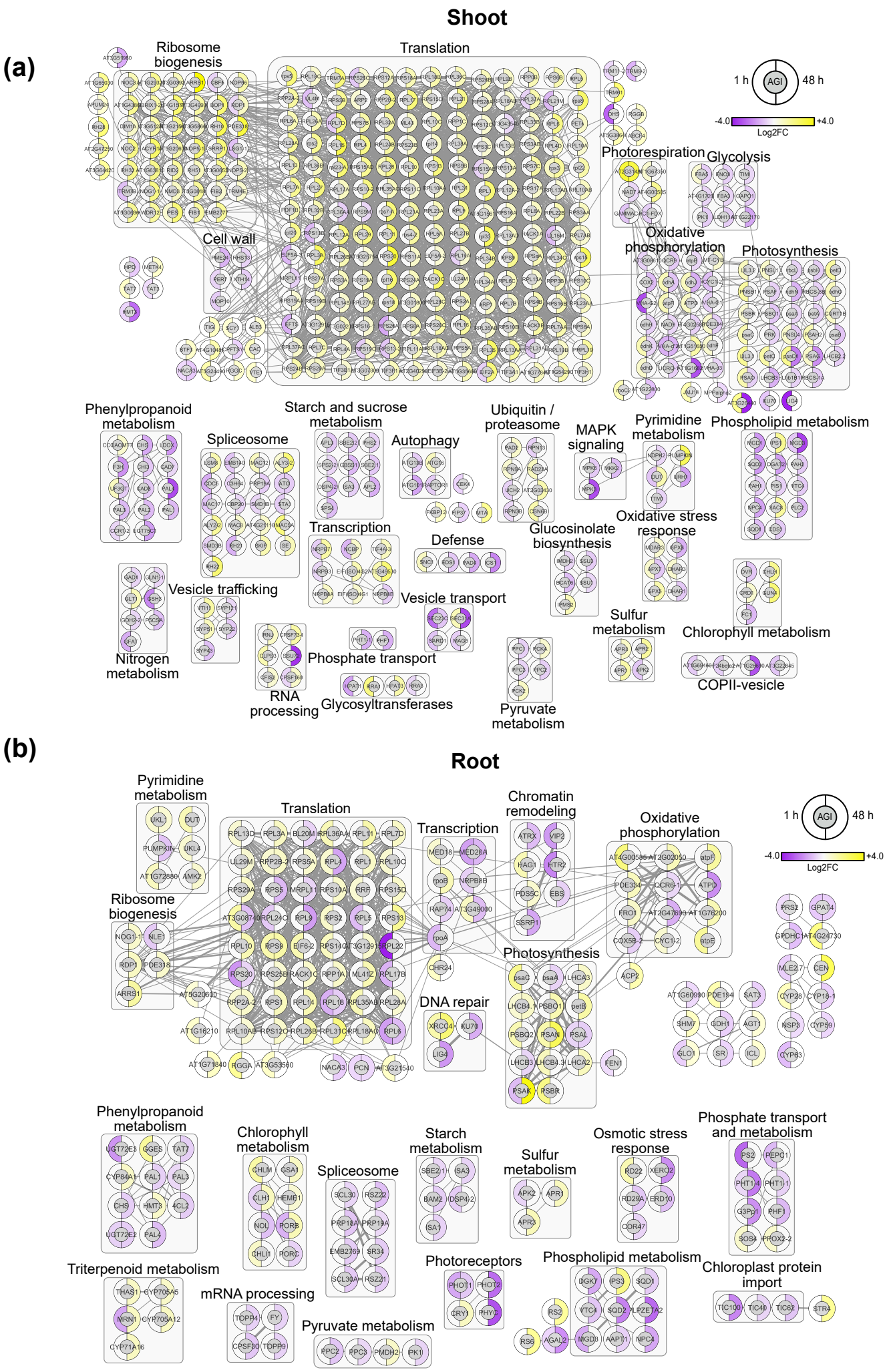

FIGURE 4 Association network analysis of proteins whose abundance changed following 1 and 48 h of Pi resupply. Association network analyses were performed using STRING-DB (ANOVA *p*-value <0.05) depicting significantly changing proteins following 1 and 48 h of Pi resupply in (a) shoots and (b) roots. Edge thickness indicates the strength of connection between nodes. Minimum edge threshold was set to 0.7 for roots and 0.9 for shoots. Node outer circles indicate the standardized relative Log2FC of the indicated protein in Pi resupply vs. -Pi. The scale of red to blue indicates relative increase and decrease in abundance, respectively. Grey circles encompass protein nodes involved in the same biological process.

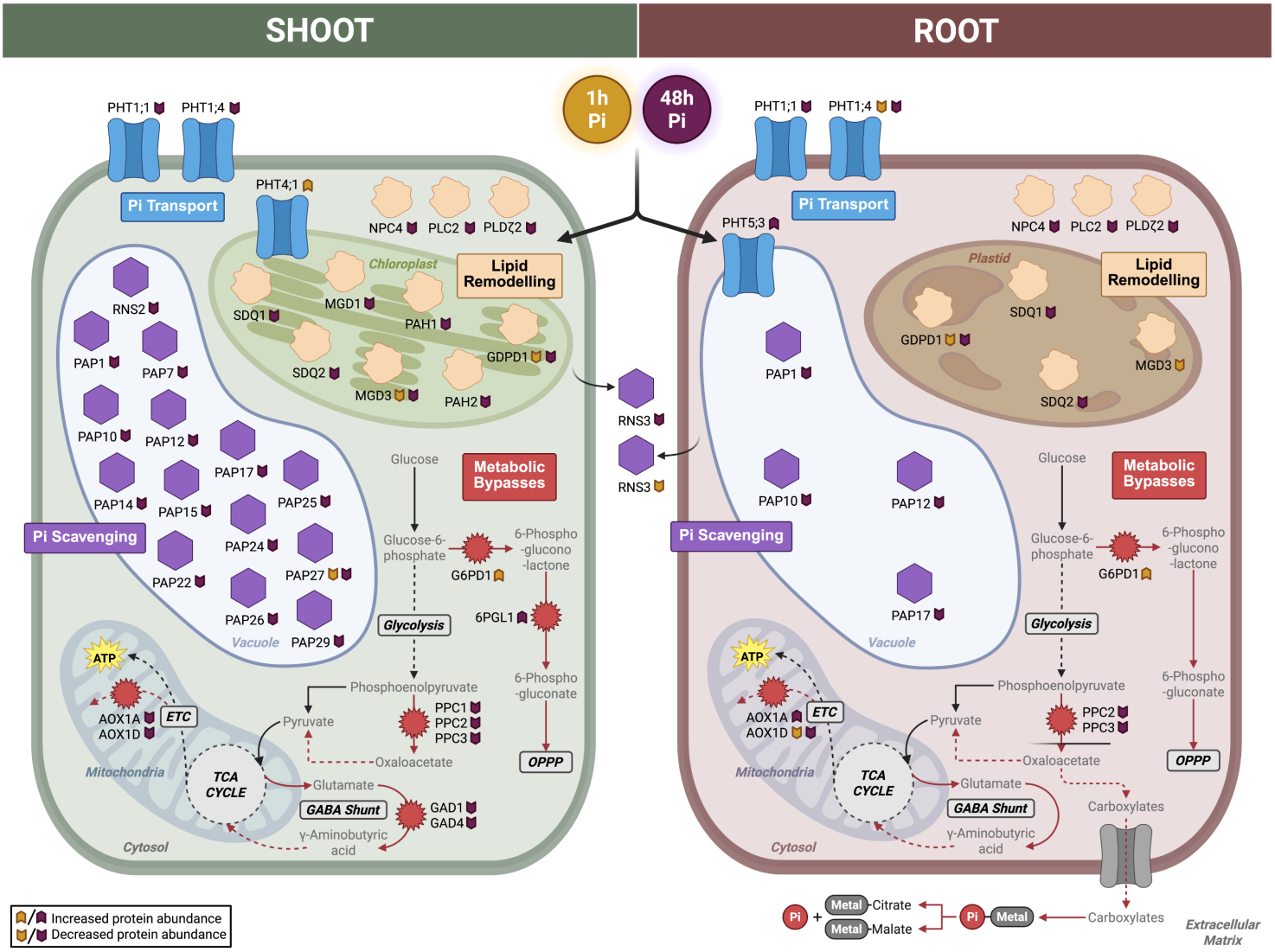

FIGURE 5 Summary of known proteomic changes observed following Pi refeeding in Arabidopsis shoots and roots. AOX, alternative oxidase; ETC, electron transport chain; GAD, glutamate decarboxylase; G6PD, glucose 6-P dehydrogenase; GDPD, glycerophosphodiester phosphodiesterase; MGD, monogalactosyldiacylglycerol synthase; NPC, non-specific phospholipase; OPPP, oxidative pentose phosphate pathway; PAH, phosphatidate phosphatase; PAP, purple acid phosphatase; 6PGL, 6-phosphogluconolactonase; PHT, Pi transporter; PL, phospholipase; PPC, plant type PEP carboxylase; RNS, ribonuclease; SDQ, sulfoquinovosyl diacylglycerol; TCA, tricarboxylic acid. Created in https://BioRender.com.

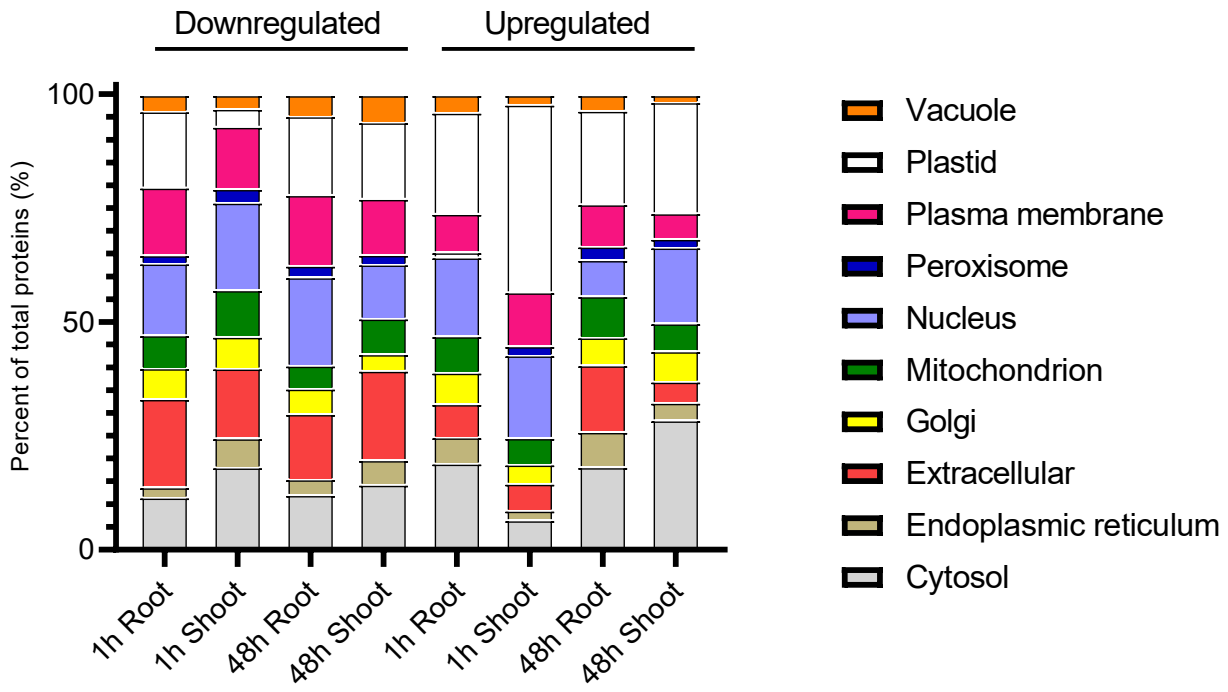

Figure S1. Subcellular localization of significantly changing proteins in Pi-resupplied *Arabidopsis* shoots and roots. *In silico* subcellular localization analysis of the significantly changing proteins that were down- or upregulated was performed using SUBAcon (https://suba.live/) for shoots and roots following 1 and 48 h of Pi resupply.

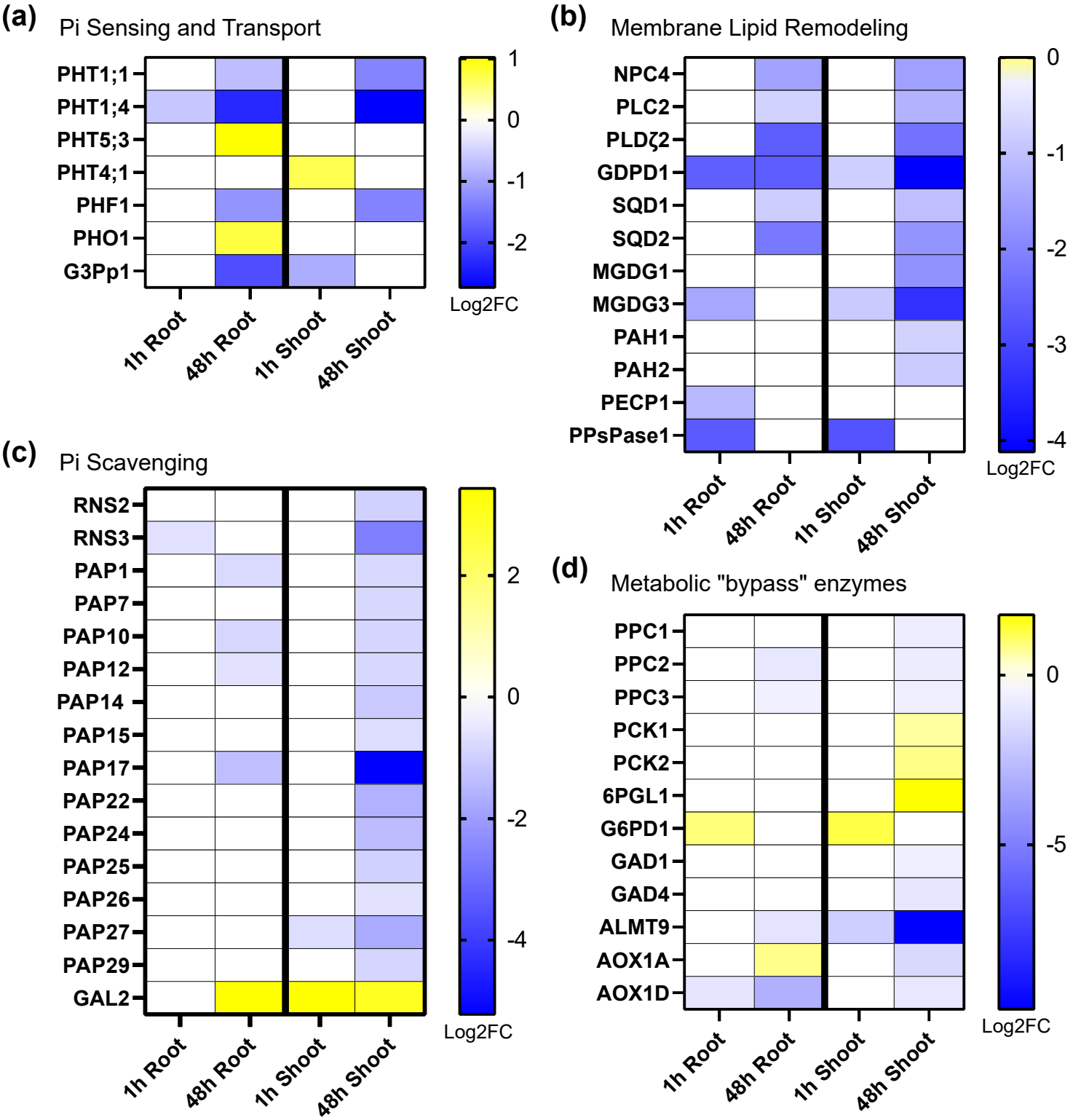

Figure S2. Summary of Pi responsive proteome. Heatmap of Pi-responsive proteome changes at 1 and 48 h after Pi resupply in shoots and roots relating to: (a) Pi sensing and transport, (b) membrane lipid remodeling, (c) Pi scavenging, and (d) and metabolic 'bypass' enzymes. Scale represents the Log2FC at the specified timepoint following Pi resupply where blue indicates downregulated and yellow indicates upregulated proteins.